EIGHT EUROPEAN ROTORCRAFT FORUM

Paper No 9.5

ACOUSTIC CAPABILITIES OF THE GERMAN - DUTCH WIND TUNNEL DNW

J.C.A. VAN DITSHUIZEN

G.D. COURAGE

R. ROSS

DNW, THE NETHERLANDS

August 31 through September 3, 1982

AIX-EN-PROVENCE, FRANCE

ASSOCIATION AERONAUTIQUE ET ASTRONAUTIQUE DE FRANCE

Summary

Aero-acoustic measurements on models in wind tunnels are becoming an essential part of the development work of future aircraft and helicopters. From the very first stage of design of the DNW the ability to perform such measurements has been included in the utility spectrum of this low speed testing facility. After extensive theoretical and experimental studies it appeared possible to realize this specific testing capability by making use of already available components of the interchangeable closed test sections (Ref. 1).

It is the aim of this paper to assess the aero-acoustic capabilities of DNW in detail.

After a short review of general features, the aero-acoustic design is elucidated, followed by an outline of the performed calibrations. The scope of applications is reviewed and several demonstration tests are described like a test on a helicopter model to determine cabin noise and a test with a jet model to evaluate the shear layer corrections. Recently an acoustic model rotor test to investigate blade-vortex interaction noise and blade slap effects has been performed. Some technical aspects of these tests are mentioned. A short elucidation is given on test data and experiences.

1. General Features of DNW

The DNW (Figure 1) is a subsonic atmospheric wind tunnel of the closed return type with three interchangeable, closed test section configurations and one open jet configuration. The interchangeable part includes three components: the contraction, the test section, and the diffusor transition. The mentioned configurations are obtained by combination of two complete sets of these components plus extra inserts for the 6x6 contraction and moveable side-walls for the convertible 8x6/6x6 test section.

The closed test sections have cross-sectional sizes of 9.5 m x 9.5 m, 8 m x 6 m, and 6 m x 6 m and maximum velocities of 62, 116, and 152 m/s respectively. The walls are provided with longitudinal slots of variable width permitting an open area ratio variation from 0 to 12%; a breather flap system allows to control the static pressure.

The open jet employs the 8 m x 6 m contraction and has a maximum velocity of 85 m/s. All test section configurations have a length of 20 m. Main design and performance data are shown in Table 1. Figure 2 shows the arrangement of the various buildings of the DNW plant. The circuit airline is shown in Figure 3.

DNW offers two standard support systems:
- a sting support system for internal balance supported models
- an external underfloor balance for strut supported models.

The sting support mechanism is shown in Figure 4. The range in angle of attack varies from -15° to $+45^{\circ}$; the range in angle of yaw from -30° to $+30^{\circ}$. Both are obtained by means of a hydraulically governed kinematic with standard rotational speeds up to 5°/s and an angle setting accuracy of $\pm .02^{\circ}$. The maximum admissible loads are shown in Table 2.

The external balance is a 6-component balance of platform type (Figure 5). The sub-structure allows for yawing models by $\pm 180^{\circ}$ with a maximum rotational speed of 1°/s and an angle setting of $\pm .1^{\circ}$. The angle of attack variations also being maximum 1°/s is normally obtained by means of a telescopic rear strut and may vary between -25° and $+65^{\circ}$ depending on the distance between the main struts and the rear strut. The maximum loads are shown in Table 3.

In addition to the standard equipment for low speed aerodynamical testing, special equipment, such as a moving belt ground plane, air turbine

powered engine simulators and a rotor support and electrical drive system are available.

The moving belt ground plane is used for realistic ground simulation (Figure 6). The design of the MBGP covers the requirements resulting from testing aircraft and helicopter models during take-off and landing in ground proximity. The dimensions are width x length: 6.3 m x 7.6 m. The belt speed ranges from 5 - 60 m/s.

The turbine powered engine simulators can be used to study aerodynamic and acoustic installation effects. Specially designed units are available for simulation of jet engine inlet and exit flow conditions up to 4000 N thrust at a typical mass flow of 3 kg/s (Figure 7) and for propeller flow field simulation up to 120 kW installed power at a typical mass flow of 1.5 kg/s (Figure 8). The drive air is delivered from the compressed air plant to the model through force-free air line bridges across the standard internal and external balance systems.

The rotor support and drive systems are capable of supporting large scale (up to Ø = 3 m) rotor rigs with a drive power up to 250 kW (400 Hz, 440 V) (Figure 9).

The DNW is equipped with two distributed computer network systems; an on-line system for controlling all tunnel components and for the acquisition and processing of data, and an off-line system for data preparation and re-processing of measured data. Post-processing of large quantities of result data is possible through a connection line to a nearby computer centre.

2. Acoustic Design Considerations

In selecting the most suitable test section configuration following aspects were considered:
- Mach number range
- Model size
- Background noise floor
- Side-line, fly-over angle range
- Frequency domain of interest

Mach number range

The highest Mach numbers for acoustic tests are determined mainly by the approach and take-off speeds of aircraft. With the expected tendency towards future configurations a velocity range of 60 to 80 m/s corresponding to Mach numbers of .175 to .235 at 0 m ISA conditions seems adequate. For the DNW this range is met by the 8 x 6 m^2 test section configuration.

Model size

The scale of noise models is generally limited by two important considerations, i.e. the ability to simulate corresponding Strouhal Numbers as at full scale, and the sensitivity of microphones in the higher frequency domain (Ref. 2). For rotary sources the rotational speed increases consequently inversely proportional with the scale of the model diameter. For 1/10th scale models this would result in typical speeds up to 35,000 rpm for a General Electric CF-6 high by-pass fan (Ø = 2.195 m) and up to 3,500 rpm for a AH-1S helicopter rotor (Ø = 14.63 m). Smaller scales would lead to unrealistic speeds, which are not considered to be feasible. For complete aircraft configuration the scale limitations may be even more severe as not all noise, e.g. boundary layer noise, scales proportional to the scale factor. Generally, however, scaling of frequency components will occur at corresponding proportionally higher frequencies at model scale.

At frequencies above 20 kHz the influence of atmospheric absorption will become increasingly important, which in combination with the threshold sensitivity of most standard microphones (¼": 60 db at 50 kHz, 1/8": 75 dB at 100 kHz) means that too high frequencies should preferably be avoided. Application of smaller scales than 1/10th for simulation of full scale frequency components up to 10 kHz, which are of importance in the PNdB-determination, seems therefore not realistic.

Hence, both aspects, noise simulation and noise measurement with the objective of making representative noise tests, limit the minimum applicable model sizes to about 1/10th of full scale. On the other hand there is also a limit to the maximum applicable model sizes based on the consideration that noise measurements shall be made in the far field to enable noise predictions to greater side-line distances than the point of measurement. The far field is characterized by noise decay following the so-called $1/r^2$-law which leads to a 6 dB attenuation with distance from the source. Extrapolations in this sense are only possible if the noise measurements are made outside the so-called near field for which the law does not hold. In practice may be distinguished between the 'acoustical" far field and the "geometrical" far field. The first usually starts some wavelengths away from the source and sets in combination with the test section dimensions a lower limit to the frequency scale in the order of 200 Hz; the second is measured by comparing the decay of multiple, interacting sources with that of a single point source of equal strength.

Figure 10 shows the result of a simplified calculation illustrating that a microphone distance of about 1.5 to 2.0 times the span of a complete model is required for reliable side-line measurements and about once the span for fly-over measurements. Similar calculations can be made for rotors. As the rotor noise is concentrated mainly near the blade tips the distance between two point sources in the example given seems a better match for the rotor diameter than a full wing span. Consequently about half the maximum applicable size results for rotor diameters. The largest applicable span based on this far field criterion would then be about 2 to 2.7 m in the closed 8 x $6_2 m^2$ test section due to the presence of the walls. In the open 8 x 6 m^2 test section configuration for which a core width of about 6 m is anticipated at the model centre location, a span up to 4 m seems realistic which requires a side-line of at least 8 m. For rotors these dimensions would be up to 1.3 m for the closed and up to 2 m for the open jet respectively. In the open jet, however, larger models may be applied if correspondingly larger side-lines are selected and no constraint is imposed by the size of the core with respect to the model near field dimensions.

Background noise floor

A major condition for execution of noise measurements in wind tunnels is that the noise floor of the tunnel does not exceed the noise generated by the model. Initially (1975), as design point for the DNW typical spectra of abt 95 PNdB of a 1/10th scale airliner were taken, measured at a 150 m side-line corresponding to FAR 36 - 10 dB. For the Mach number range considered this resulted in a 1/3 OBSPL requirement of 85 dB at 1,000 Hz at 80 m/s. However, as during the design of the DNW a tendency was observed that more stringent requirements might be put forward, it was decided to aim at airframe noise levels during approach instead. Figure 11 shows an estimate of the expected DNW level based on corrected model tunnel data resulting in a 1/3 OBSPL of 73 dB at 1,000 Hz.

Side-line angle range

In practice it will be desirable to measure the emitted noise at other locations than for maximum emission angles. Fan noise and airframe

noise are known to be dominant in the forward quadrant up to 40°. Rotor noise may even show directivities up to 30° (Ref. 3). Jet noise is particularly dominant in the rearward quadrant between 130° and 150°. This requires that the microphone measuring range shall extend preferably from 30° to 150° whereby the noise floor shall be lower than 73 dB preferably.

Frequency domain of interest

The frequency range of interest is directly related to the model scale. The upper limit is set more or less by the type of microphones. For PNdB determination the lower limit is set by the lowest 1/3 octave band centre frequency at full scale, i.e. 50 Hz. As this contribution is low generally and standard 1/4" microphones are preferred the frequency range required for a 1/10th scale model should be between 1,000 Hz and 50 kHz. For other, more specific applications like source directivity analyses, even lower frequencies down to 100 Hz may apply, e.g. in case of rotor tests.

Choice of test section configuration

In case of a closed test section it is not feasible to place the microphones in the walls as the boundary layer generated noise (80 m/s 116 dB at 1,000 Hz typical) will exceed the desired background noise floor. In-flow microphones on the other hand are known to have also rather high wind induced noise levels (80 m/s: 90 dB at 1 kHz, 85 dB at 10 kHz typical) which are even increased by the unavoidable presence of nose cones. Consequently by using commercially available microphones a strong preference is present for measurements outside the tunnel flow.

A further important aspect is that the measured noise signals should be free from spurious effects due to wall reflections. In order to keep the reflection contributions within a reasonably low value, say .5 dB, a simple analysis by means of ray acoustics using virtual sources as mirror images shows that an absorption coefficient of at least .9 is required. For the desired frequency range this is not compatible with the closed test section requirement of aerodynamically smooth walls. The remaining choice is then to use special, often complex, measuring techniques or eliminate the walls completely and provide a reflection poor testing hall around an open jet configuration.

Although noise measurements in a closed test section environment are possible, the open jet configuration was considered to be the most promising solution for far-field measurements. A proper location of microphones in the testing hall requires distances from the model of half to once the test section width for fly-over and once to twice the test section width for side-line positions. To obtain an anechoic environment the walls, ceiling and floor of the testing hall shall be covered with noise absorbing material.

3. Aero-Acoustic Configuration

Description

The open jet configuration consists of the exchangeable 8 x 6 m^2-configuration at the upstream side and the exchangeable transition part of the 9.5 x 9.5 m^2 test section at the downstream side. The free length of the open jet amounts to 20 m. The testing hall surrounding the open jet measures some 45 m length, 30 m width and 20 m height. A sketch of the basic lay-out of the testing hall is shown in Fig. 12 while a picture is shown in Fig. 13.

For the execution of far field noise measurements outside the flow five microphones are mounted on a traversing rig which is located along

one of the side walls of the testing hall. This rig can as a whole be moved in a lateral direction to establish the required side-line measurement distance. The microphones can further be traversed continuously in flow direction during the tests in order to collect test data over a complete sideline. In addition to these traversing microphones several microphones are mounted at fixed positions near the ceiling and at extreme sideline positions. All microphones are provided with wind spheres and are directed towards the model centre. The geometrical range covered by the microphones at the nearest side-line varies from 25^{o} to 160^{o}.

All walls of the testing hall are covered with sound absorbing material in order to minimize sound reflections. For about 40% of the surface this sound absorbing material consists of wedges of 0.8 m high (absorption-coefficient 0.99 and cut-off frequency 80 Hz). The remaining 60%, from which sound signals can only reach the microphones through secondary reflections, is covered with flat material of 0.2 m thickness (absorption-coefficient 0.9 and cut-off frequency 200 Hz).

Design aspects

Major consideration in designing the open jet configuration was to get sufficiently low background noise levels at stationary flow conditions up to at least 80 m/s with a jet of sufficient length to provide the desired sideline angle range. Although initial model tunnel tests gave promising results, several measures (1, 2), which were already incorporated in the aerodynamic design were reviewed and after an extensive series of tests a number of others (3, 4, 5) were incorporated. Basically following measures apply:

1. selection of a low number of revolutions of the fan (n_{max} = 225 rpm) resulting in a relatively low tip Mach number of the fan blades (Ma = .5)
2. selection of a sensible ratio of the number of rotor and stator vanes of the fan (8:7)
3. application of forward and backward sweep of the nose cone support struts and stator vanes respectively
4. acoustic treatment of the vanes in the first and fourth corner as well as the inside of the 9.5 x 9.5 m^2 transition
5. application of a low resistance, reflection poor and acoustically treated collector/transition.

The first three measures aim at a low noise generation at the fan itself. According to Lighthill the total acoustic power varies with the sixth degree of the local approach velocity. As the fan drive speed was already chosen low in order to avoid compressibility effects and thus strive for high aerodynamic efficiency a further improvement did not seem realistic in view of the increased blade loading this would bring with the increased danger of fan stall. Hence, a further reduction was not considered feasible.

Theoretical studies to find the optimum rotor stator configuration showed that complete suppresion of pure tone fan noise at blade passing frequency may be achieved by selecting a stator vane number of 11 at 8 rotor blades. For structural reasons however this figure was not acceptable and the original number of 7 had to be maintained. However, as the the major contribution to the pure tone fan noise generation is the periodic rotor blade wake impingement on the stator vanes (or vice versa), some suppression can also be achieved by sweeping and leaning of the stator vanes to cope with the phase shift in both radial and tangential direction of the rotor blade wakes. The same principle holds for the nose cone support struts. As leaning is rather unattractive from a structural point of view, however, only sweep was applied to the full scale stator vanes and strut supports. The selected angle for each is 15^{o}, backward and forward respectively.

Acoustic treatment of the turning vanes to reduce the fan noise propagation to the test section was studied experimentally. The DNW turning vanes are sheet metal vanes of 90° arc with 10% chord extensions. Noise tests in a 1/5th scale corner model without flow showed, that inside treatment is far more efficient for noise reduction than outside treatment. Treatment of the 1st and 4th corner of the model tunnel, leaving constant area passages between adjacent vanes, gave reductions of test section noise levels up to 17 dB and 6 dB respectively at 2.5 kHz and speeds up to 85 m/s. The best treatment for the DNW defined by these experiences was to consist of an outer layer of perforated plate (30% open, Ø = 2,5 mm holes), 1 cm thick filter material to prevent contamination and a filling of glass wool in prefabricated packages. In addition rounded-off leading edges were used to smooth in the lining with the vanes.

Collector design is based on the consideration that reflection of noise emitted by models towards microphones should be minimal and noise production itself as low as possible. This resulted in a semi-ellipsoidal, streamlined contour with a relatively small frontal area. Among the model configurations tested finally the combination 8 x 6 m^2 contraction and 9.5 x 9.5 m^2 transition with an open jet of 20 m long proved to be satisfactory. Stable flow conditions were reached by application of a slot for air exchange at the downstream end of the collector/transition.

Lining of both collector and transition was considered necessary to prevent sound reflections back into the testing hall and attenuate boundary layer diffusor noise propagating towards the test section. The collector/transition is basically treated in a similar way as the turning vanes having 20 cm thick glass fibre packages underneath a 1 cm thick filter mat and covered with perforated plate. Additional treatment is applied to the collector's outer side by bonding filter material to the perforated plate to get rid of hissing noise caused by the flow over the holes.

4. Calibration Tests

In the framework of the calibration of DNW tests were performed to assess the aero-acoustic quality in detail. These tests comprise the determination of the anechoic properties of the testing hall, the aerodynamic characteristics of the open jet, the background noise level of the open jet and the correction procedures for the passage of noise through the shear layer inclusive atmospheric absorption.

Anechoic properties

A simple criterion to check the anechoic quality of a hall is the so-called $1/r^2$-law. In essence this law says, that noise propagating from a point source decays in such a manner that doubling the distance from the source causes a reduction of the noise level by 6 dB after accounting for atmospheric attenuation. Reflections from surrounding walls may cause deviations from this regular pattern and may in case of pure tones for instance lead to standing waves.

The testing hall of DNW has been checked with respect to $1/r^2$-law. This part of the activities has been taken care of by DFVLR and the results have been reported in Ref. 4.

Three different noise sources were used to cover the complete range of frequencies of interest for future testing:

- a low frequency loudspeaker for the frequency range of 50 Hz to 1,000 Hz
- a so-called dodecahedron (twelve loudspeakers grouped together as a dodecahedron and rotating about a vertical axis) for the frequency range of 200 Hz to 4,000 Hz

- an airball with pinholes for the frequency range of 5,000 Hz to 40,000 Hz.

Both latter noise sources were provided by the Boeing Noise Technology Laboratory. The noise sources were located near the centre of the open jet section. The loudspeaker systems could generate both pure tones and wide band noise, while the airball from its very nature could generate only wide band noise.

Measurements of the radiated noise were made by microphones supported from the standardly available traversing rig, thus covering the area of most interest for future tests. In contrast with the standard streamwise movement, the traversing rig was moved to and from the tunnel centre line while the microphones remained at a fixed longitudinal position.

The tape recorded discrete frequency microphones signals were passed through a 1/3 octave band filter and a subsequent amplifier and then plotted as SPL-traces versus the traverse position on an X-Y plotter (Figures 14 to 16). For each test condition 10 level traces corresponding to 10 microphone traverse paths, are assembled in a summary plot. To facilitate comparison the theoretical curves - corresponding to the $1/r^2$-decay - are drawn in as dashed lines, thus providing an indication of the spatial distribution of the interference pattern, i.e. the difference between the maxima and the minima of the standing wave pattern with respect to the ideal curve. The shown ideal slopes are corrected, however, for atmospheric attenuation and source directivity effects.

The tests revealed that the anechoicness of the testing hall of DNW meets reasonably high standards. With broadband noise excitation of rather low frequency (up to some 1,000 Hz) and filtering the microphone signals at a 1/3-octave band with centre frequency at 400 Hz, the results as shown in Figure 14 are obtained. No trace of waviness can be observed and only some irregularities occur at the far extrimity of the test area due to shielding of the 9,5 x 9,5 m^2 collector. Increasing the frequency to really high values (31,500 Hz) even further improves the result as can be seen from Figure 15. Only in case of pure tone excitation with rather low frequency (400 Hz) some evidence of standing waviness is present (Figure 16). This specific situation will in practice, however, seldom occur.

Aerodynamic Characteristics

The quality of a jet stream is characterized by stationary and non-stationary criteria. The first may be categorized in axial flow deviations and flow angularity. Figure 17 shows the spatial distribution in kinetic pressure in one specific cross-section as measured by a pitot-static probe attached to the sting support mechanism at two velocities, 40 m/s and 70 m/s. The results show that at this cross-section, i.e. the model centre which lies 7 m downstream of the 8 x 6 m^2 contraction exit, the core height measures about 5 m. This corresponds to an angle of 'influence' for the shear layer, i.e. $\frac{\Delta q}{q} \gtrsim 2\%$, of about 4 degrees with respect to the lipline. For the larger part of the core the deviations in q are less than 0.5%, but amount to 1% near the periphery.

Similar conclusions may be drawn by observing the incidence flow angularity in the vertical plane of symmetry. The angular deviation is generally less than $\pm .1^o$ for both angle of incidence and of yaw, except for the influence region of the shear layer which becomes manifest at a point about 2.5 m underneath the centre line of the tunnel (Fig. 18).

The non-stationary flow quality is presented in the form of the rms turbulence intensity as obtained with a plane X-wire attached to the sting support (Ref. 5). Figure 19 shows the variation of the longitudinal and lateral components with wind speed at the model centre. The longitudinal component is clearly less monotonic, obviously influenced

by the shear layer eddy mechanism. Nevertheless the measured values may be characterized as low for open jet facilities. Moreover a frequency analysis of the recorded signals showed, that the main energy is contained in the very low frequency range (50 Hz).

Figure 20 shows the spatial variation of the longitudinal and the two lateral components in the region of interest as defined by the kinetic pressure measurements. The influence of the shear layer becomes manifest in the interaction of the various components, e.g. the longitudinal and vertical components in the vertical plane of symmetry tend to become equally large. Near the "corners" all components are more or less equal.

Inside the region of "constant" kinetic pressure substantial variations of the measured turbulence intensities may be observed, say from 0.15% at the centre line to 1.5% near the corners. In spite of this the results make it clear that there is a core of about 5 m wide and 3 m high in which the turbulence intensities remain smaller than 0.5%.

Background Noise Properties

Background noise, often called the "noise floor", is the total microphone signal in the absence of the noise source being tested. The background noise includes noise from extraneous sources (such as wind tunnel drive system, fan, and flow noise), and noise generated by flow over the microphone. Background noise must always be measured during a test to assure an adequate signal-to-noise ratio for the test measurements being made. Typically, the noise floor is recorded for each microphone, installed in its test position, as the noise floor can vary with microphone position relative to extraneous sources.

Inside the flow

The noise floor of a microphone (with aerodynamic nose cone) installed in a wind tunnel flow is relatively high compared to out-of-flow microphones for two reasons:

1) The microphone is near extraneous sources generated by the wind tunnel
2) The flow over the microphone nose cone generates noise which is sensed as part of the noise floor. Boeing studies (Ref. 6) have shown that the microphone self-noise is proportional to flow turbulence intensity as well as near flow velocity. The relatively low turbulence in the DNW appears to minimize self-noise, as illustrated in Fig. 21, where the in-flow noise floor is compared with the nominal self-noise as published by Brüel & Kjaer.

Therefore the measured in-flow background noise comprises microphone self-noise (primarily at the higher frequencies) as well as noise from extraneous sources (Fig. 22). It should be noted, however, that the in-flow microphone is very close to the source being tested. Therefore, the in-flow signal-to-noise ratio is much better than would be inferred from a comparison of measured in-flow and out-of-flow background noise levels.

Outside the open jet flow

Outside the tunnel flow the air velocities are small, and no wind-induced noise is present when a foam spherical wind screen is used. The background noise spectra, measured 12.2 m from the tunnel centre line and at a typical model overhead position are given in Fig. 23 for three wind tunnel speeds. The noise floor distributions, measured along a 12.2 m sideline, parallel to the tunnel flow are given in Fig. 24.

From the spectra it can be seen that the noise concentrates at the lower frequency range and gradually decreases towards the higher frequencies. This effect is in agreement with the fact, that the cut-off frequency of the acoustical treatment of the testing hall is in the range

of 100 - 200 Hz. Something can be said about the actual sources of background noise in this wind tunnel. From personal observations in the hall, which are confirmed by the spatial distribution of the noise levels, it can be concluded that the main noise source in the testing hall at high speeds is the boundary layer flow along the trailing edge of the nozzle exit. Although not clear in Fig. 23, some high frequency noise, directed upstream, is heard from the flow collector and from the perforated walls further downstream inside the diffusor.

Even at the maximum windspeed of 80 m/s the overall background noise level is extremely low. Comparison of this level with the estimate based on the design studies shows a considerable improvement at frequencies below 1 kHz while at 10 kHz the results match. At 2 and 5 kHz the real levels are underestimated slightly depending on the directivity with respect to the source position. Airframe noise testing in take-off or landing configuration should therefore fall well within the capabilities of this tunnel.

Shear Layer Characteristics

The effect of the shear layer on sound propagation was checked in a co-operative programme between DNW, Boeing, NLR and DFVLR (Ref. 7). A noise source model, developed and calibrated by Boeing was used. The model was provided with a set of multitone horns, and an acoustic driver coupled to a horn for single pure tones and broadband noise generation (Figure 25). Far field directivities inside and outside of the flow were obtained. In-flow data were extrapolated to the out-of-flow sideline using a spherical divergence and atmospheric absorption correction. The Amiet (Ref. 8) shear layer correction for infinitely thin shear layers and an atmospheric absorption correction were used for the out-of-flow acquired noise data.

A typical example of the results obtained with these tests is presented in Figure 26. These data refer to a 1/3 octave band analysis with a centre frequency at 4000 Hz and a tunnel speed of V = 65 m/s. The in-flow data have been decreased with 23 dB to account for the shift from the 0.61 m sideline (in-flow) to the 8.6 m sideline (out-of-flow). As can be seen the results coincide almost perfectly over the complete angular range, which means that the correction applied to the out-of-flow results meets the requirements very well. At higher frequencies however, differences were found which could not be explained by spectral broadening, refraction or scattering due to turbulence. Spectral broadening was checked by narrow band analysis up to pure tones of 12.5 kHz with and without flow. The broadening was indeed found to be smaller than the particular 1/3 octave frequency band (Ref. 9). Refraction according to the infinitely thin shear layer theory was verified by using a Boeing developed programme for phase differences measured with closely space microphones at 90° and rearward angles up to frequencies of 8 kHz at 80 m/s. At forward angles, the angle corrections were verified using correlation techniques for in-flow and out-of-flow microphones comparisons of broadband noise. Directivity scattering due to turbulence did not occur for strongly directive noise sources up to a frequency of 30 kHz. However, at forward angles, where a steep increase in SPL magnitude corrections is calculated (assuming an infinitely thin shear layer). SPL corrections were found to be too large at high frequencies and high tunnel velocities ($>$ 8 kHz at 80 m/s).

Figure 27 shows the thus established flight effects for in-flow and out-of-flow measurements In contrast to the results obtained with the scale model facility, which has a proportionately thin shear layer, at rearward emission angles there were indications of absorption of sound waves by the turbulence at high frequencies and tunnel speeds. This was supported by the fact that sound energy was lost at all rearward angles. Furthermore, at 80 m/s tunnel speed, flow effects limit the side-

line/fly over measurable source directivity angles to a range of 45^{o} to 155^{o}. Testing outside this range requires additional measures like in-flow testing or selecting a microphone side-line very close to the shear layer.

5. Scope of Applications

The results of the performed calibrations make clear that the DNW open jet configuration disposes of an excellent flow quality which combined with very low background noise levels and good anechoicness of the testing hall permits aero-acoustic testing of complete 1/10th scale or larger models and components up to at least 4 m span or 2 m rotor diameter. Large models may be applied, however, as no constraint is imposed by the size of the core with respect to the model near field dimensions. Generally, models with these dimensions should be well within the potential core as established by kinetic pressure and turbulence measurements. The calibrations further showed that for out-of-flow noise measurements the infinitely thin shear layer corrections have to be modified to account for turbulence effects for high speed (> 40 m/s) and high frequency (> 8 kHz) conditions. Using this modified procedure enables accurate out-of-flow measurements up to 40 kHz and emission angles between 45^{o} and 155^{o} with respect to the model. For inflow measurements, if applicable, holds that the signal to noise ratio must be large enough to overcome spurious effects like wind induced noise on the microphones or noise from extraneous sources as supports etcetera.

With the known background noise levels it is possible to analyse the application of the DNW in a number of cases. Typical examples of airframe configurations or components are shown in Figure 28. This makes clear that for airframe noise measurements a sufficiently large margin is available. Another example is shown in Figure 29, which illustrates the available margin for a 1/7th scaled down helicopter model.

6. First Tests and Outlook

Helicopter Cabin Noise

Already in 1979 first acoustic measurements were executed by the DFVLR Technical Acoustics Department with a rotor model on the DFVLR rotor test rig in the DNW (Figure 30). The tests served to determine in detail the instationary pressure field on a cabin model for coherence analyses and internal overal sound pressure levels in the framework of similar flight tests with the DFVLR Bo 105_2helicopter (Ref. 10). The tests were conducted in the closed 8 x 6 m^2 test section, which inspite of the presence of the hard, unlined walls, proved to have a sufficiently low background noise level. A typical spectrum of main rotor noise under forward flight conditions measured by a microphone positioned at the contraction exit is shown in Figure 31.

Jet Noise

Annex to the acoustical calibration of the DNW open jet configuration an evaluation of the DNW shear layer correction procedure was made together with the Boeing Noise Technology Laboratory and the NLR Propulsion and Acoustics Department using a $\emptyset$ = 6 cm hydrogenperoxide propulsive model jet (Figure 32). The evaluation was done by comparing in-flow and fully corrected out-of-flow flight effects on jet noise (Ref. 11). After appropriate smoothening of SPL and flight effect data it was found that the application of the additional correction significantly improved the in-flow/out-of-flow comparisons. A typical example is shown in Figure 33.

The results were further compared to the Boeing data base comprising full scale F-86 flight and jet model tunnel (NASA 80' x 40', Boeing 7' x 7') data and were found to produce the highest flight effects indicating that the DNW jet model was the cleanest configuration tested. For jet noise dominated conditions, static throttle line/flight data relationships (SPL versus relative velocity) show good agreement between the DNW and the data base results, however.

Rotor Noise

In a co-operative programme between the Aeromechanics Laboratory of the U.S.Army Research and Technology Laboratories, the DFVLR Technical Department and DNW, a two bladed 1/7th geometrically scaled model of the AH-1G/OLS main rotor was utilized to conduct an acoustic experiment in the open jet configuration. The main focus of the test program was to investigate the sources and scalability of impulsive noise due to blade-vortex interaction and high forward speed flight. Conditions were chosen to match previously run full scale test conditions in which acoustic data were gathered by an in-flight measurement technique developed by the Aeromechanics Laboratory (Ref. 12). Figure 9 shows the set-up in the open jet. The model rotor rig as supplied by the Aeromechanics Laboratory was supported by a tower construction. In-flow microphones, positioned at corresponding flight positions, were supported by partly ligned, streamlined poles, also supported by the tower construction. The good open jet flow quality is illustrated in Figures 34 and 35 showing single and averaged records of microphone signals ahead of the rotor during a half and of a leading edge lower surface absolute pressure transducer during a full rotor revolution respectively. The nearly identical time histories of the instantaneous and the averaged data are clearly obvious, thus lessening the need for averaging. The averaged data, while better in overall character tend to smear the higher frequency details which can be clearly seen to very high frequency resolution (up to 20 kHz) because of the basic steadiness of the operating conditions.

Figure 36 at last, shows an example of a high speed impulsive noise recording by a microphone located directly ahead of and in the plane of the rotor. Shock-like pressure disturbances are radiating similar to those measured in full scale testing under similar non-dimensional test conditions (Ref. 13). The nearly identically time histories of the averaged and unaveraged microphone data support the use of DNW for high-speed acoustic research.

Outlook

First tests and calibration of the DNW have shown its ability to perform reliable and representative aero-acoustic measurements on both jet models and rotor models, both in-flow and out-of-flow. It was demonstrated further that the measured background noise levels are low enough, and the side-line angle range large enough to cope with aero-acoustic testing on large scale airframe noise models and rotor models supported by suitable clean supports. This ability puts DNW well forward in the field of aero-acousting testing.

References

1. F. Jaarsma, M. Seidel, The German-Dutch Wind Tunnel DNW - Design Aspects and Status of Construction. Paper No. B3-07, 11th ICAS Congress, Lisbon, Sept. 10-16, 1978.

2. W.B. de Wolf, Possibilities for Aero-Acoustic Investigations in the LST 8x6. NLR TR 73130U, Oct., 31, 1973 (in Dutch).

3. F.H. Schmitz, D.A. Boxwell, S. Lewy, C. Dahan, A Note on the General Scaling of Helicopter Blade-Vortex Interaction Noise. Paper presented at the 38th Annual Forum of the American Helicopter Society, Anaheim, California.

4. K.J. Schultz and K.-H. Spiegel, Acoustic Calibration of the German-Dutch Wind Tunnel - Anechoic Quality of the DNW Test Hall. DFVLR-Institutsbericht IB-128-81/7, 1981.

5. U. Michel, E. Froebel, Turbulence Levels in the German-Dutch Wind Tunnel. DFVLR Institutsbericht IB-22214-82/B2, Jan. 1982.

6. K.J. Young, Noise Characteristics of a 1/4 inch Brüel & Kjaer Microphone with a UA 0385 Nose Cone in Airflow. Paper presented at AGARD Meeting, March 15, 1979, NASA Ames, California.

7. R. Ross, J.W.G. van Nunen, K.J. Young, R.M. Allen, and J.C.A. van Ditshuizen, Aero-Acoustic Calibration of DNW Open Jet. DNW TR 82.03, (also Boeing Document D6-51501), July 1982, NOP, Netherlands.

8. R.K. Amiet, Correction of Open Jet Wind Tunnel Measurement for Shear Layer Refraction. AIAA Paper No. 75-532, 1975.

9. R. Ross, Spectral Broadening Effects in Open Wind Tunnels in Relation to Noise Assessment. AIAA Journal, Vol. 19, No. 5, pp. 567 - 572, May 1981.

10. K.-J. Schultz, Aero-acoustic Wind Tunnel Measurements with the DFVLR Helicopter Rotor Test Facility in the DNW. TN-80-SM/TA-4 (DFVLR), 1980.

11. W.H. Herkes, F.G. Strout, R. Ross and J.C.A. van Ditshuizen, Acoustic Evaluation of DNW Shear Layer Correction using a model Jet. DNW TR 82.04, (also Boeing document D6-51502), July 1982, NOP, Netherlands

12. F.H. Schmitz and D.A. Boxwell, In-Flight Far Field Measurement of Helicopter Impulsive Noise. Journal of the American Helicopter Society, Vol. 21, No. 4, Oct. 1976.

13. F.H. Schmitz and Y.H. Yu, Theoretical Modeling of High-Speed Helicopter Impulsive Noise. Journal of the American Helicopter Society, Jan. 1979.

TYPE OF TUNNEL	CLOSED RETURN CIRCUIT (OVERALL LENGTH OF CENTERLINE: 320 m)		
SIZE OF WORKING SECTION	9.5 x 9.5	8 x 6	6 x 6
TYPE OF SECTION	CLOSED	CLOSED AND OPEN	CLOSED
CONTRACTION RATIO	4.8	9.0	12.0
MAX. SPEED (m/s)	62	116 (85)	152
STATIC PRESSURE IN TEST SECTION	ATMOSPHERIC (1 BAR)		
REYNOLDS NUMBER $\times 10^{-6}$ *)	3.9	5.2	5.8
MAIN DRIVE	THYR. SYNCHR. MOTOR: NORMAL RATING: 12.7 MW		
AUXILIARY DRIVES	MAINLY FOR COMPR. AIR; ≈7 MW		
FAN	SINGLE STAGE; 8 BLADES; DIRECT DRIVE 225 RPM; CONST. PITCH, WIND SPEED CONTROL BY MOTOR		

*) BASED ON V_{max} AND 0.1 $\sqrt{A}$ (A: TEST SECTION AREA)

Table 1: Main Design and Performance Data

	MAXIMUM ADMISSIBLE LOADS
AXIAL FORCE	+ 12500 N ÷ - 7500 N
TRANSVERSAL FORCE	+ 12500 N ÷ - 12500 N
VERTICAL FORCE	+ 35000 N ÷ - 15000 N
ROLLING MOMENT	+ 15000 Nm ÷ - 15000 Nm
PITCHING MOMENT	+ 14000 Nm ÷ - 14000 Nm
YAWING MOMENT	+ 12000 Nm ÷ - 12000 Nm

Table 2: Maximum admissible loads of the sting support system

	MAXIMUM ADMISSIBLE AERODYNAMIC LOADING
DRAG	+ 20000 N ÷ - 20000 N
SIDEFORCE	+ 20000 N ÷ - 20000 N
LIFT	+ 65000 N ÷ - 65000 N
ROLLING MOMENT	+ 20000 Nm ÷ - 20000 Nm
PITCHING MOMENT	+ 40000 Nm ÷ - 40000 Nm
YAWING MOMENT	+ 35000 Nm ÷ - 35000 Nm

Table 3: Maximum admissible aerodynamic loading of the external balance

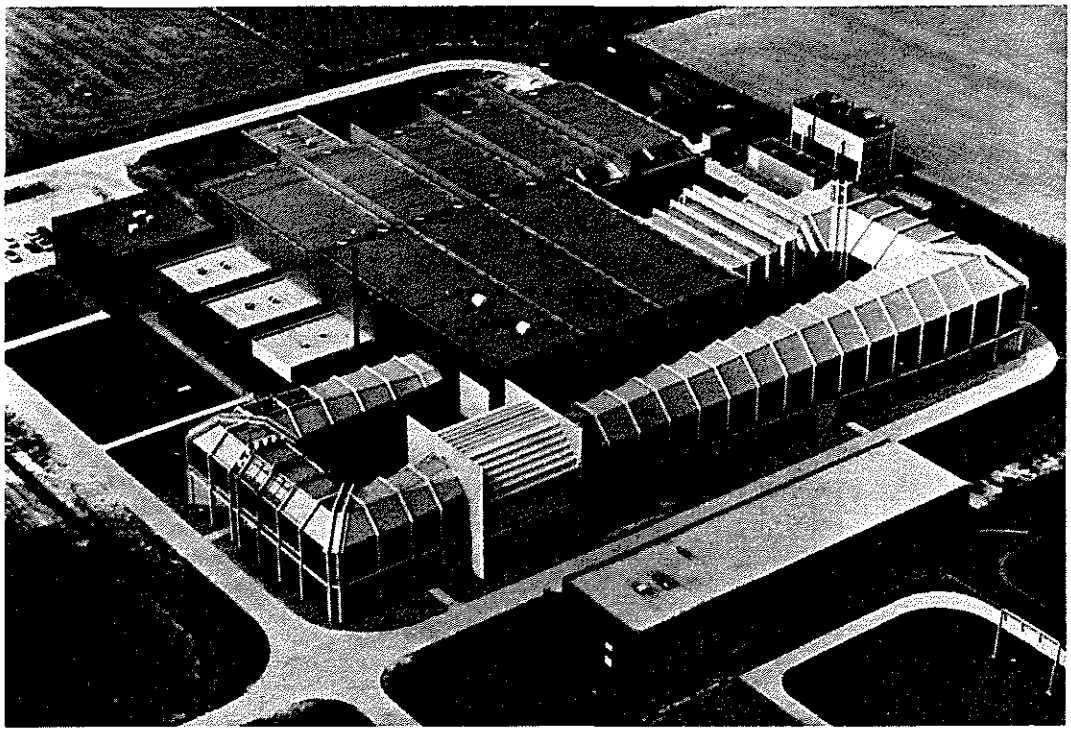

Fig. 1 Aerial view of DNW

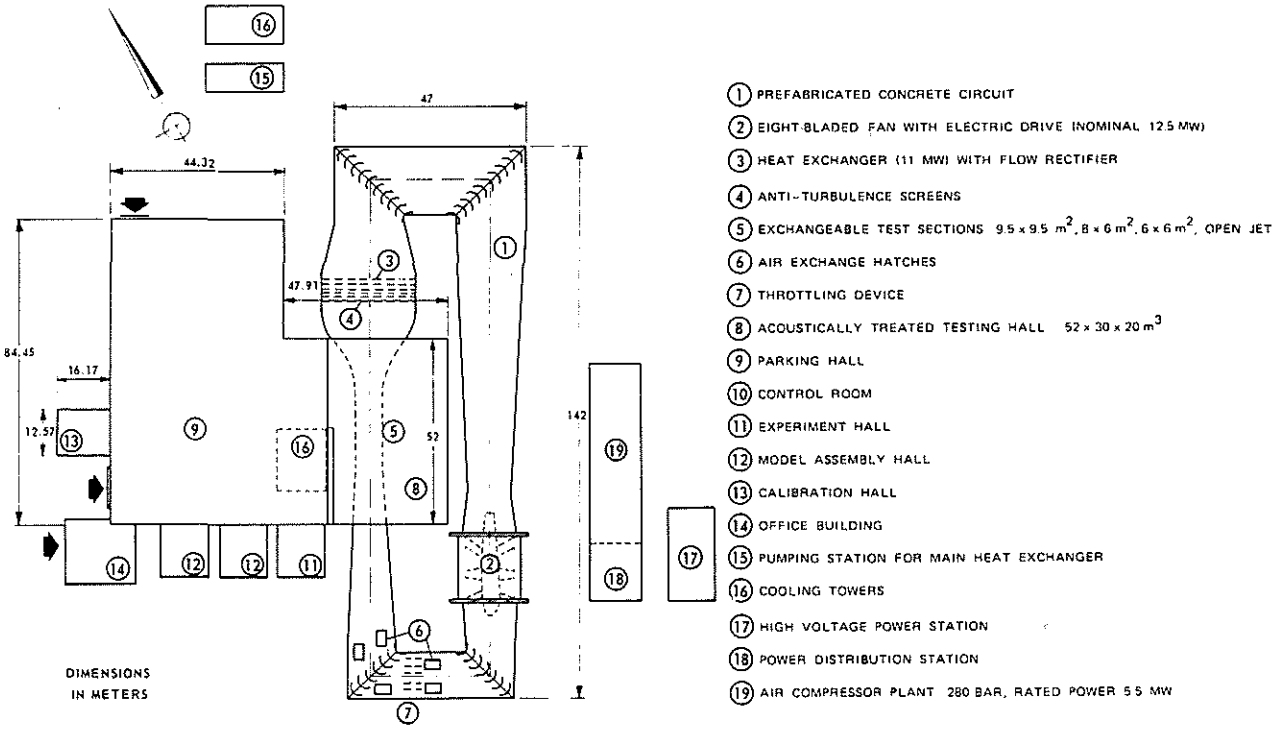

Fig. 2 Plant arrangement

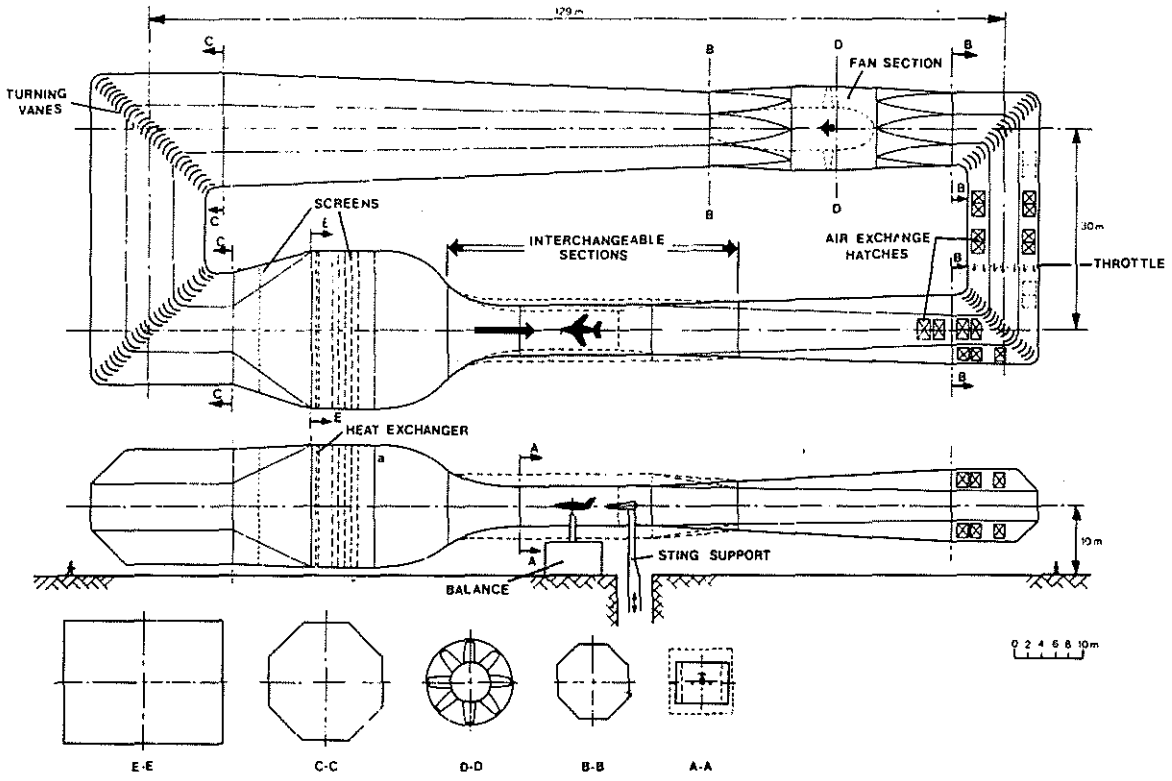

Fig. 3 Circuit airline

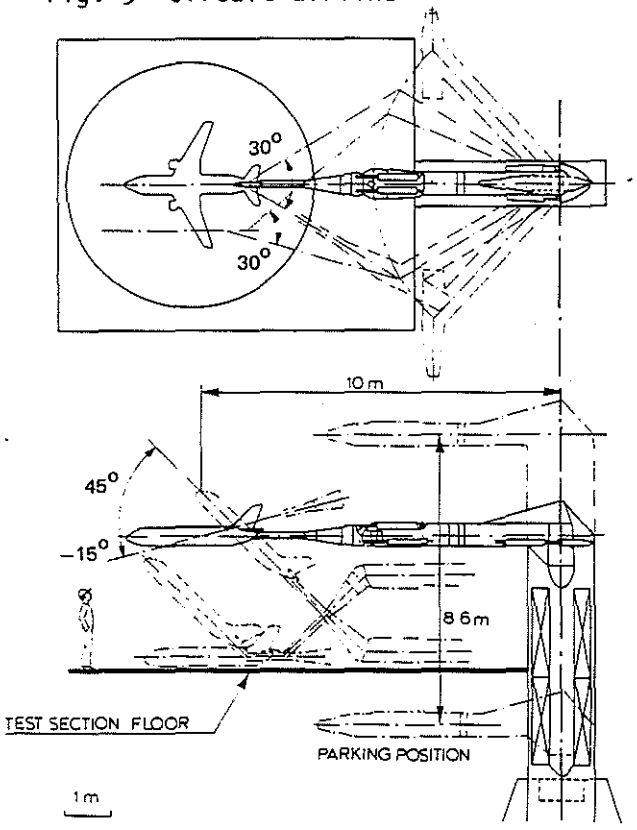

Fig. 4 Sting support mechanism

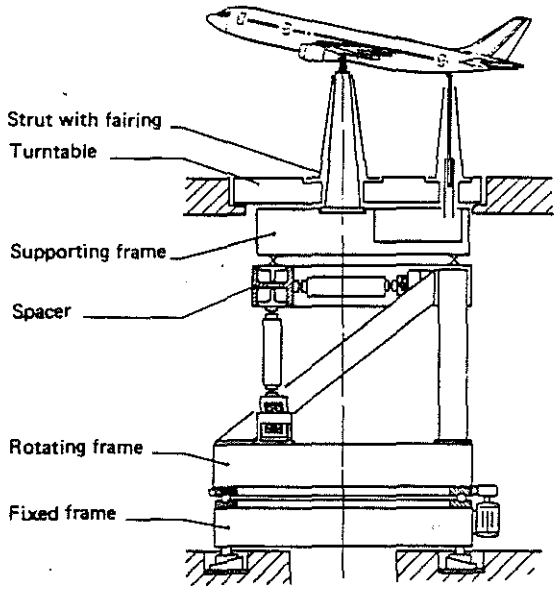

Fig. 5 External balance with full model support

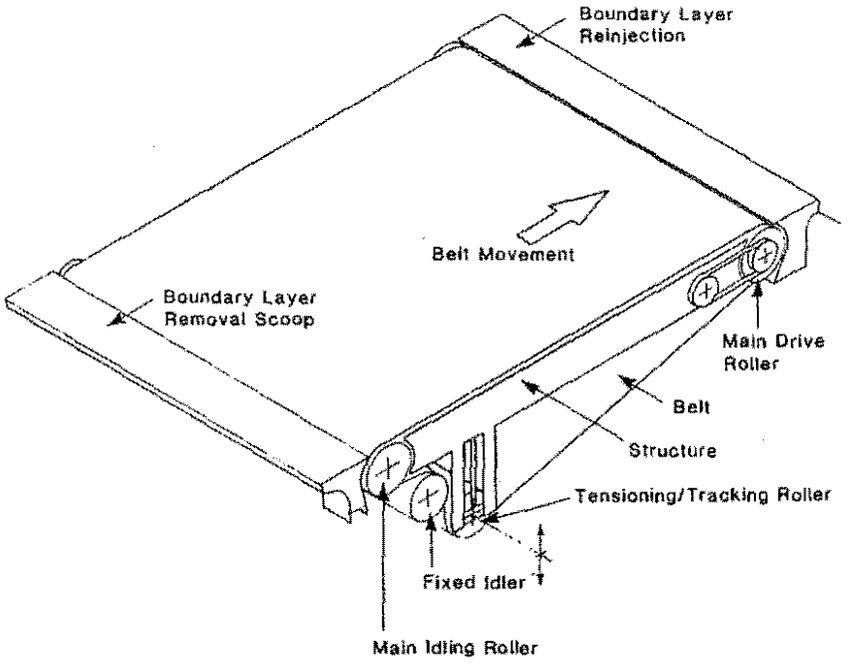

Fig. 6 Moving belt ground plane schematic

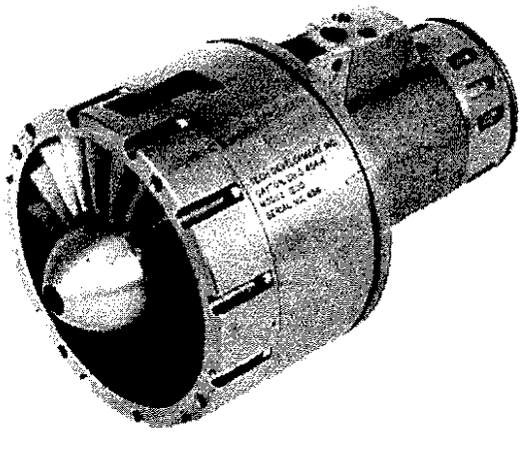

Fig. 7 Turbo powered engine simulator

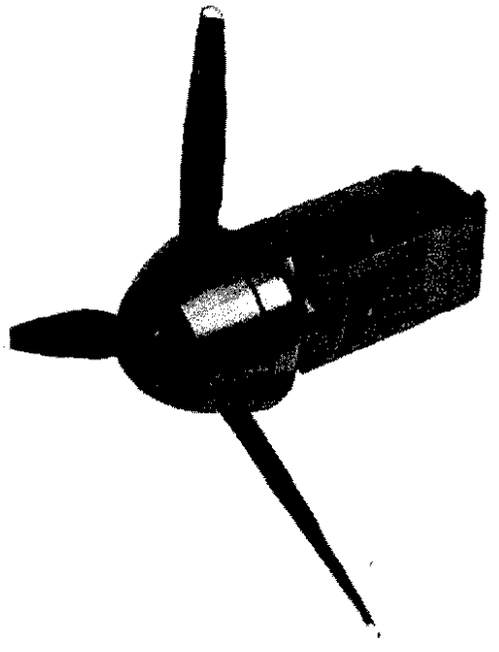

Fig. 8 Turbo prop engine simulator

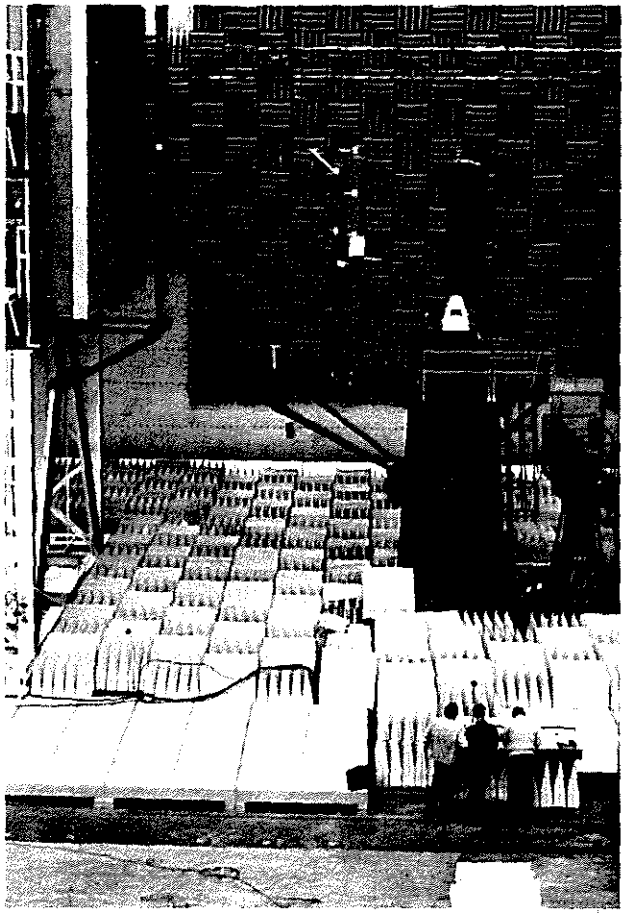

Fig. 9 Rotor support

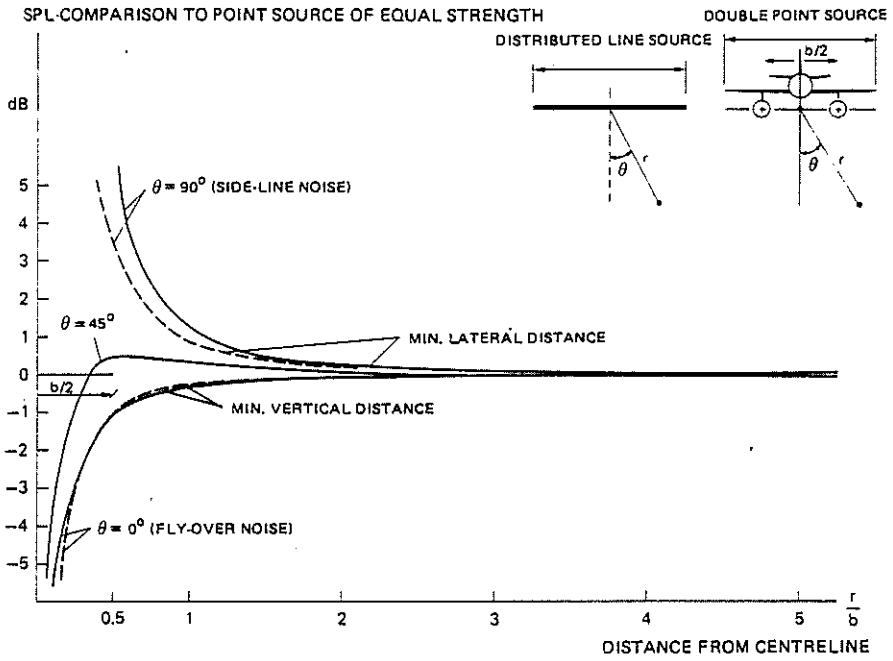

Fig. 10 Geometric near field effects from multiple sources

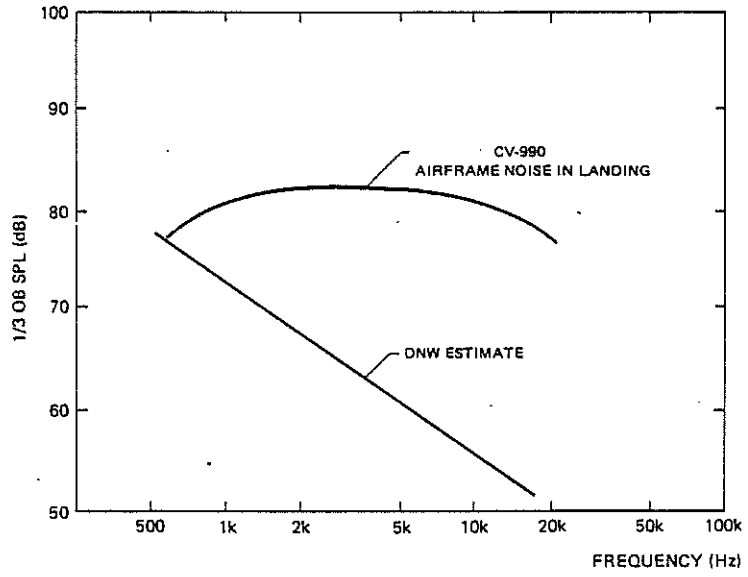

Fig. 11 Comparison of estimated background noise level versus typical airframe noise level at scaled 150 m sideline

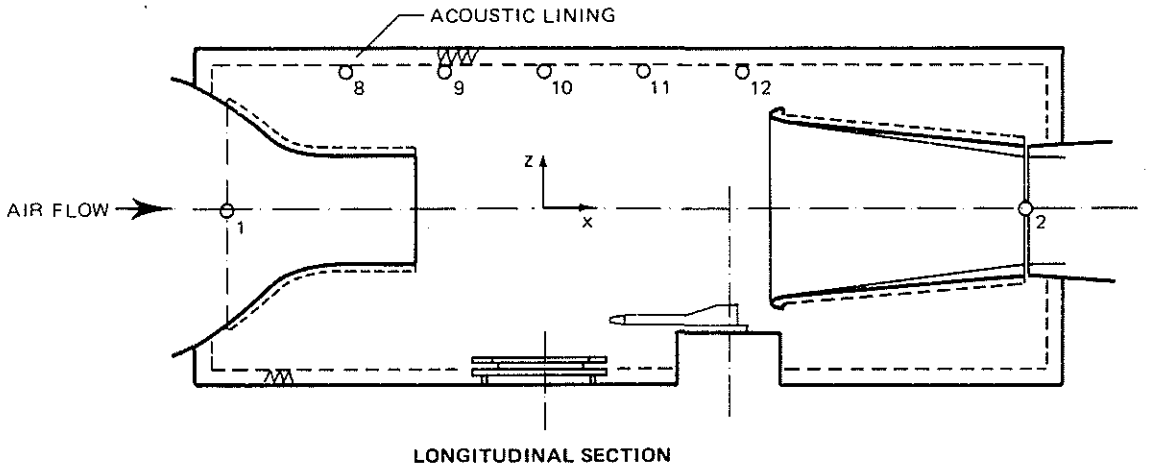

Fig. 12 Open test section configuration

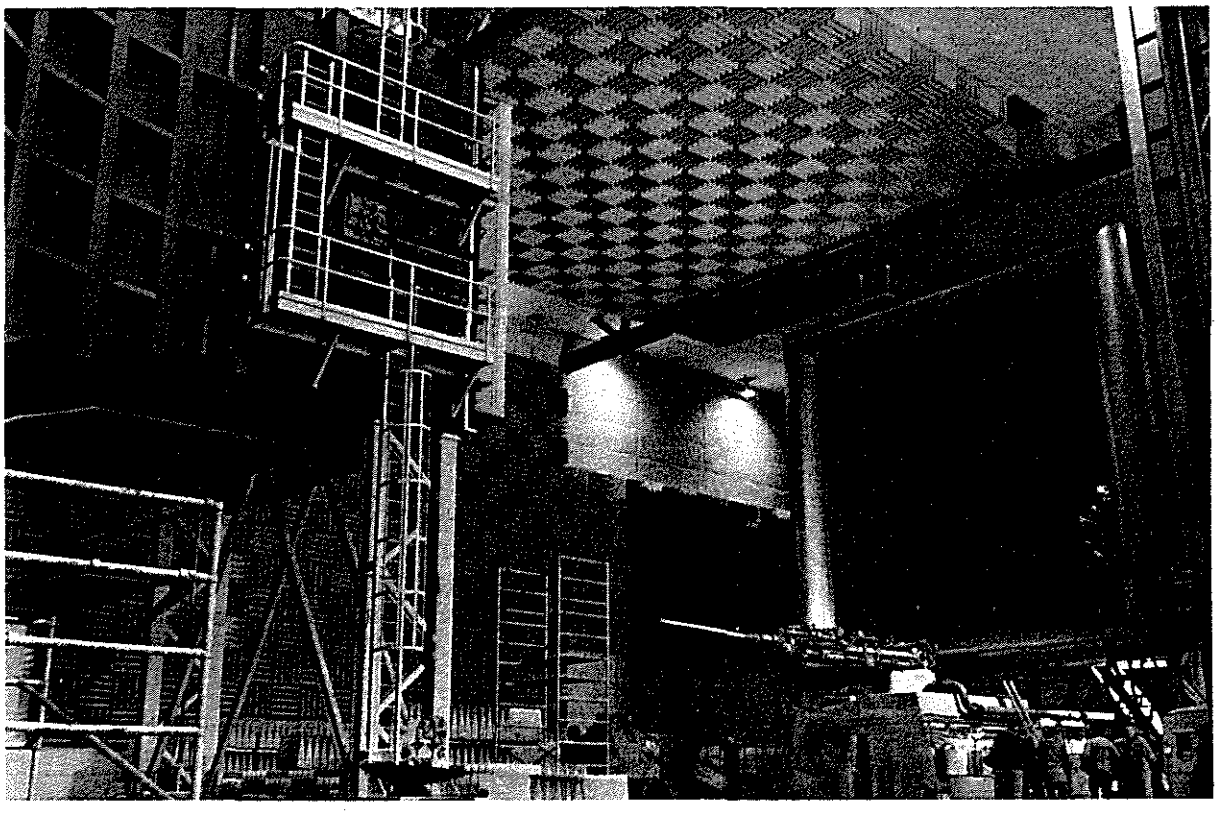

Fig. 13 View of the open jet configuration together with sting support and anechoic test hall

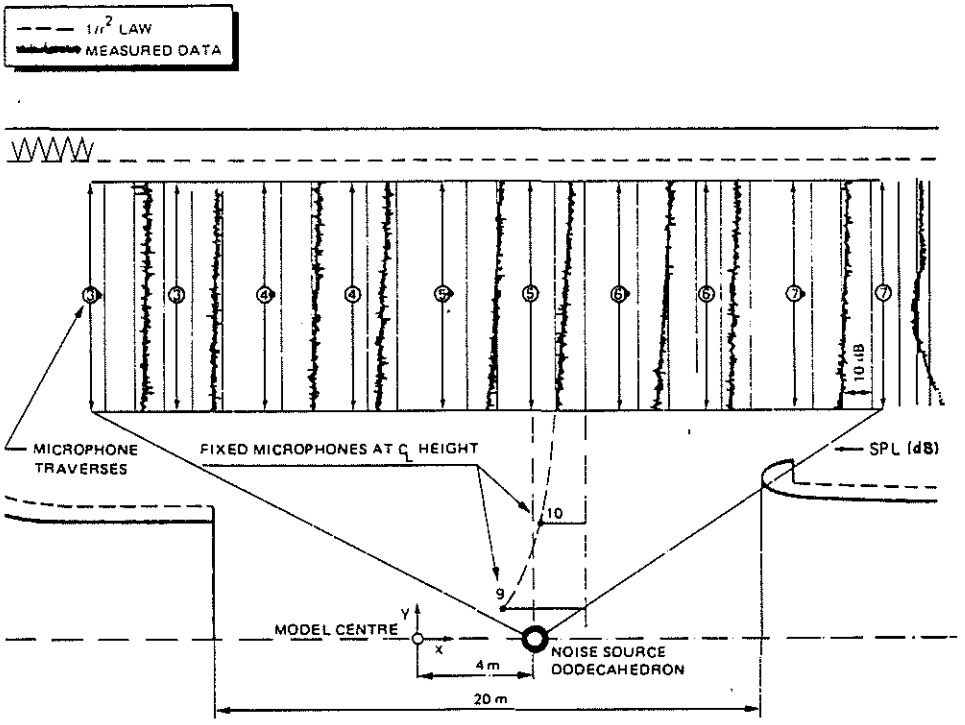

Fig. 14 $1/r^2$-law test with broadband excitation (1/3 OB/400 Hz)
③ : mic. number (see fig. 12)

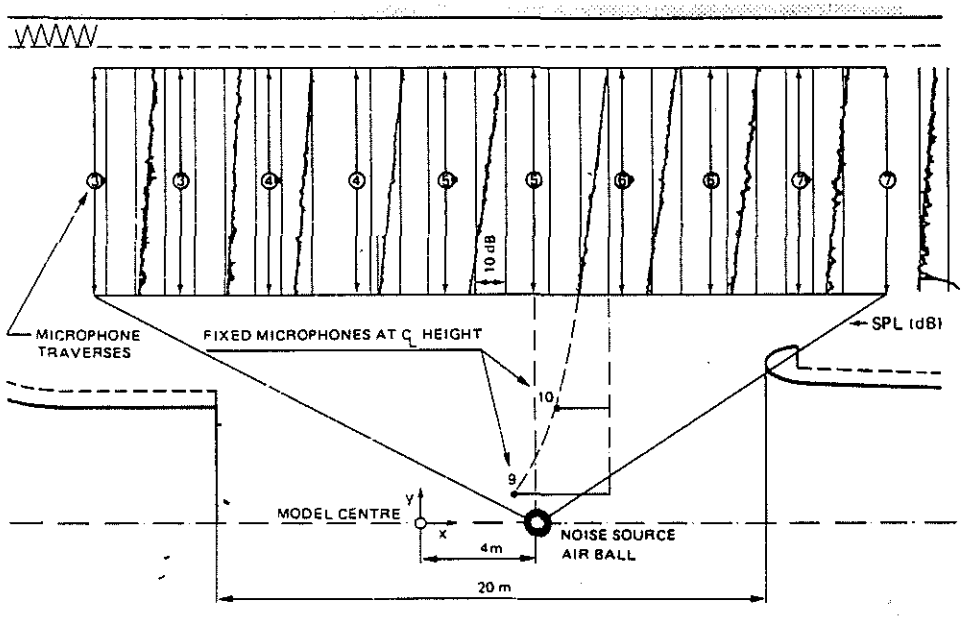

Fig. 15 $1/r^2$-law test with broadband excitation (1/3 OB/31.5 Hz)
③ : mic. number (see fig. 12)

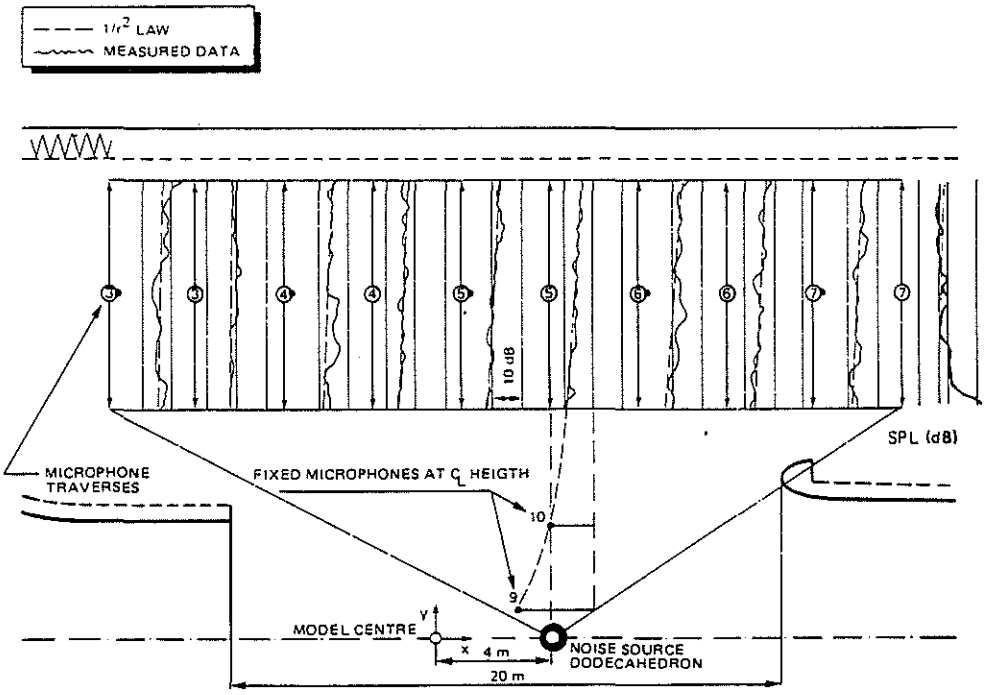

Fig. 16 $1/r^2$-law test with source tone excitation (1/3 OB/400 Hz)
③: mic. number (see fig. 12)

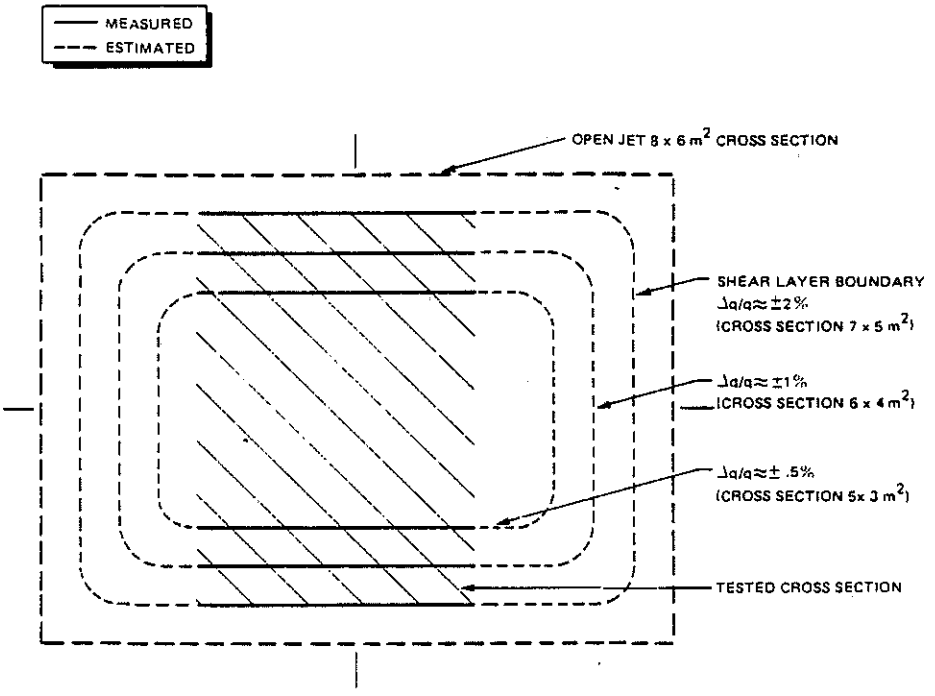

Fig. 17 Spatial variation of kinetic pressure at 40 m/s and 72 m/s

a) ANGLE OF INCIDENCE

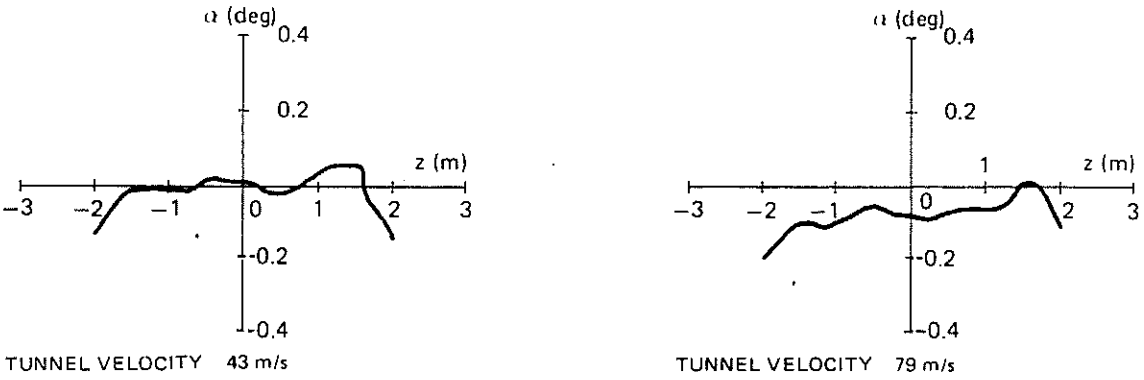

b) ANGLE OF YAW

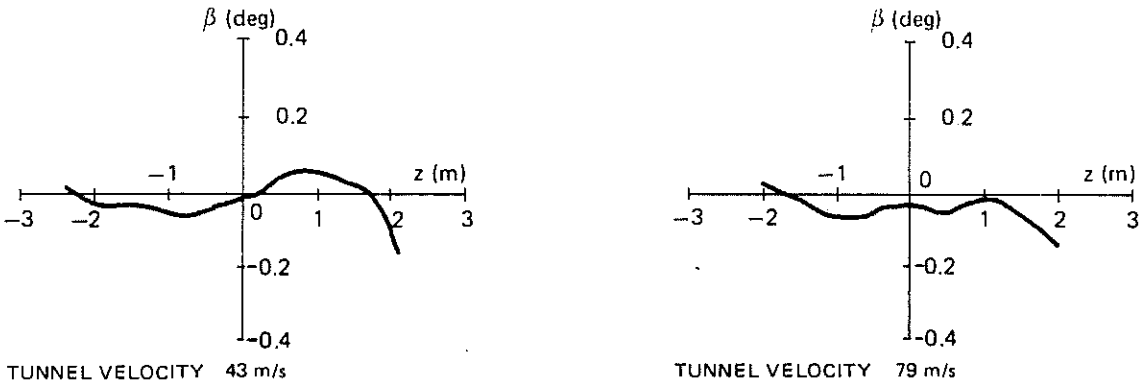

Fig. 18 Variation of angle of incidence and of yaw

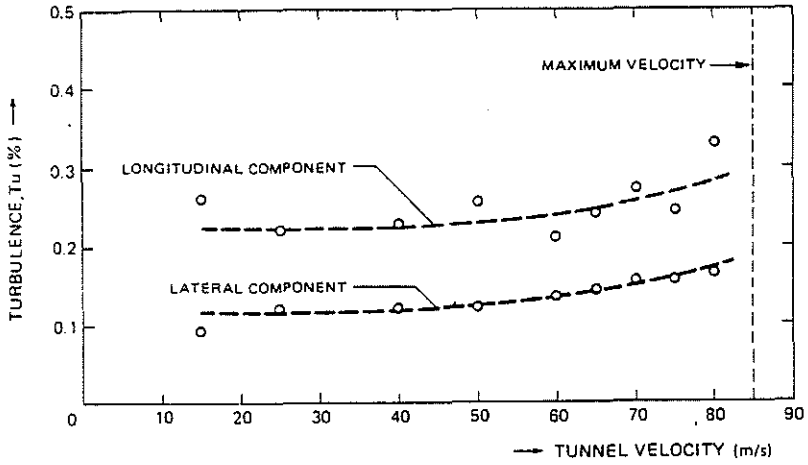

Fig. 19 Hot wire measured rms turbulence intensity

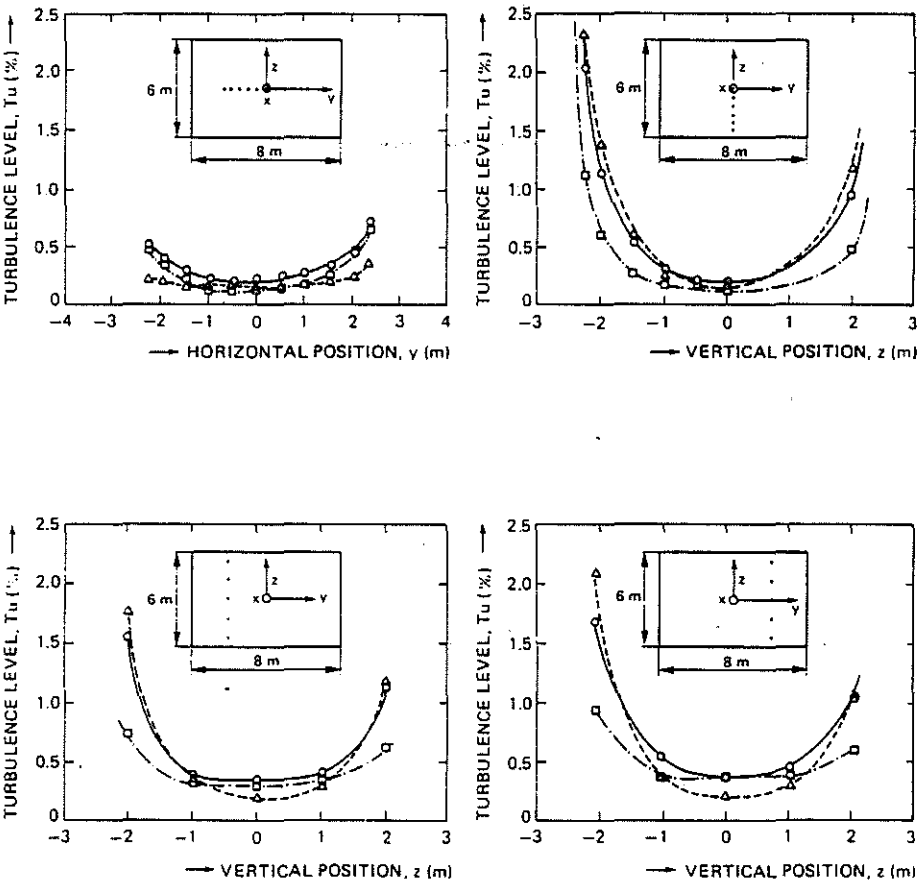

Fig. 20 Longitudinal (o), vertical (Δ) and horizontal (□) rms velocity fluctuations

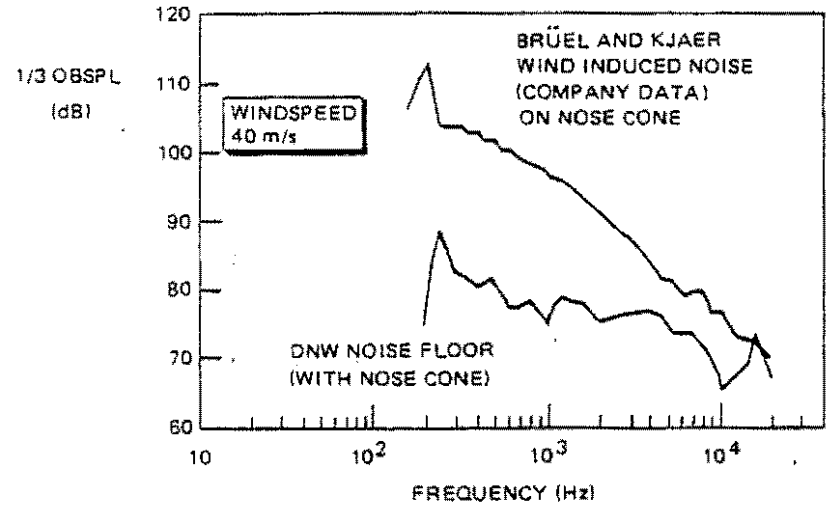

Fig. 21 DNW in-flow noise floor compared to B&K company data

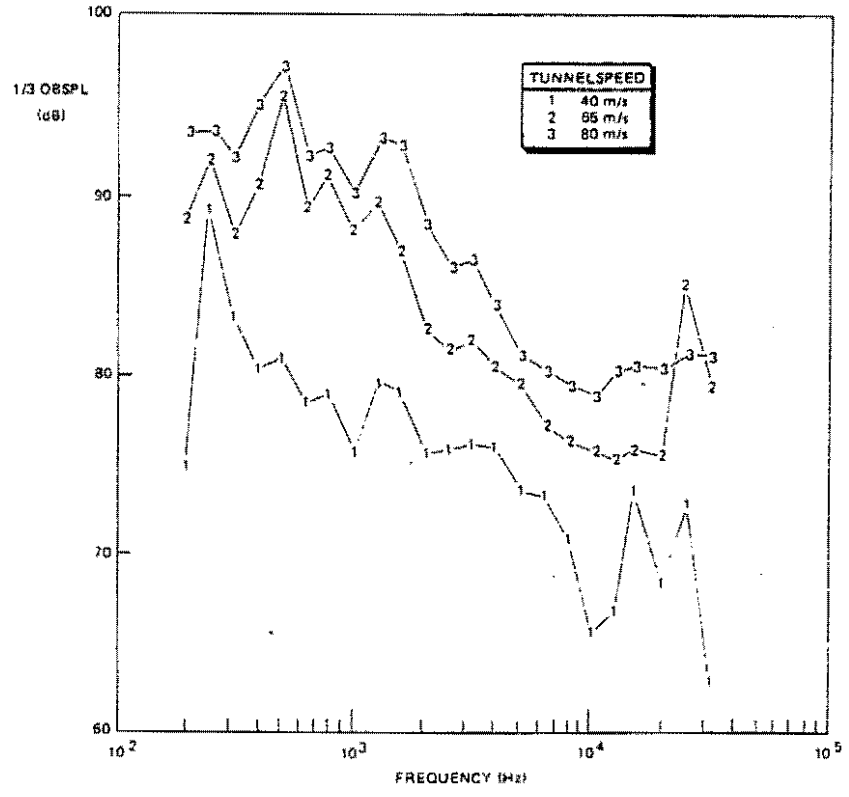

Fig. 22 In-flow noise-floors at 3 windtunnel speeds using Bruel & Kjaer nose cone on ¼" microphone

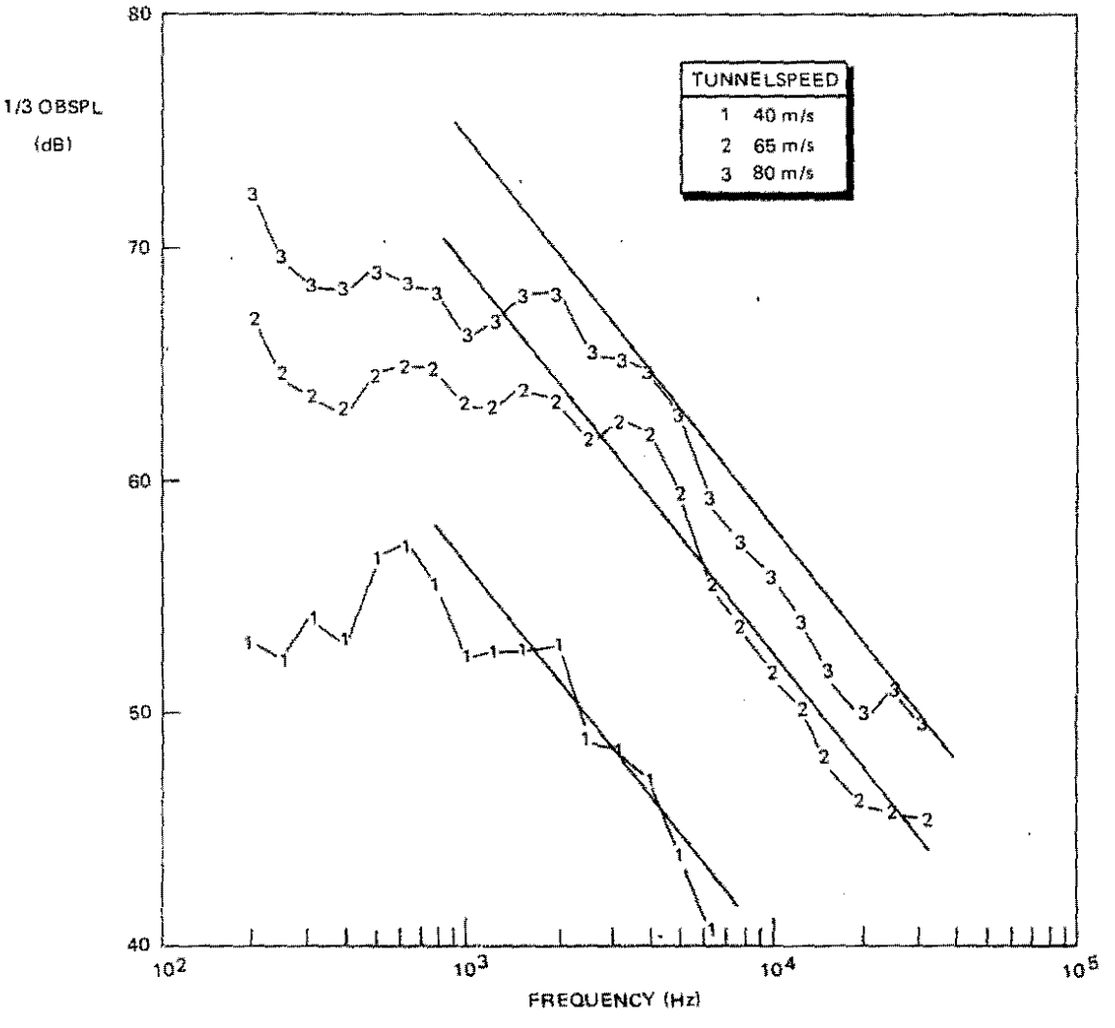

Fig. 23 Out-of-flow (12.2 m sideline) noise floors at 3 windtunnel speeds

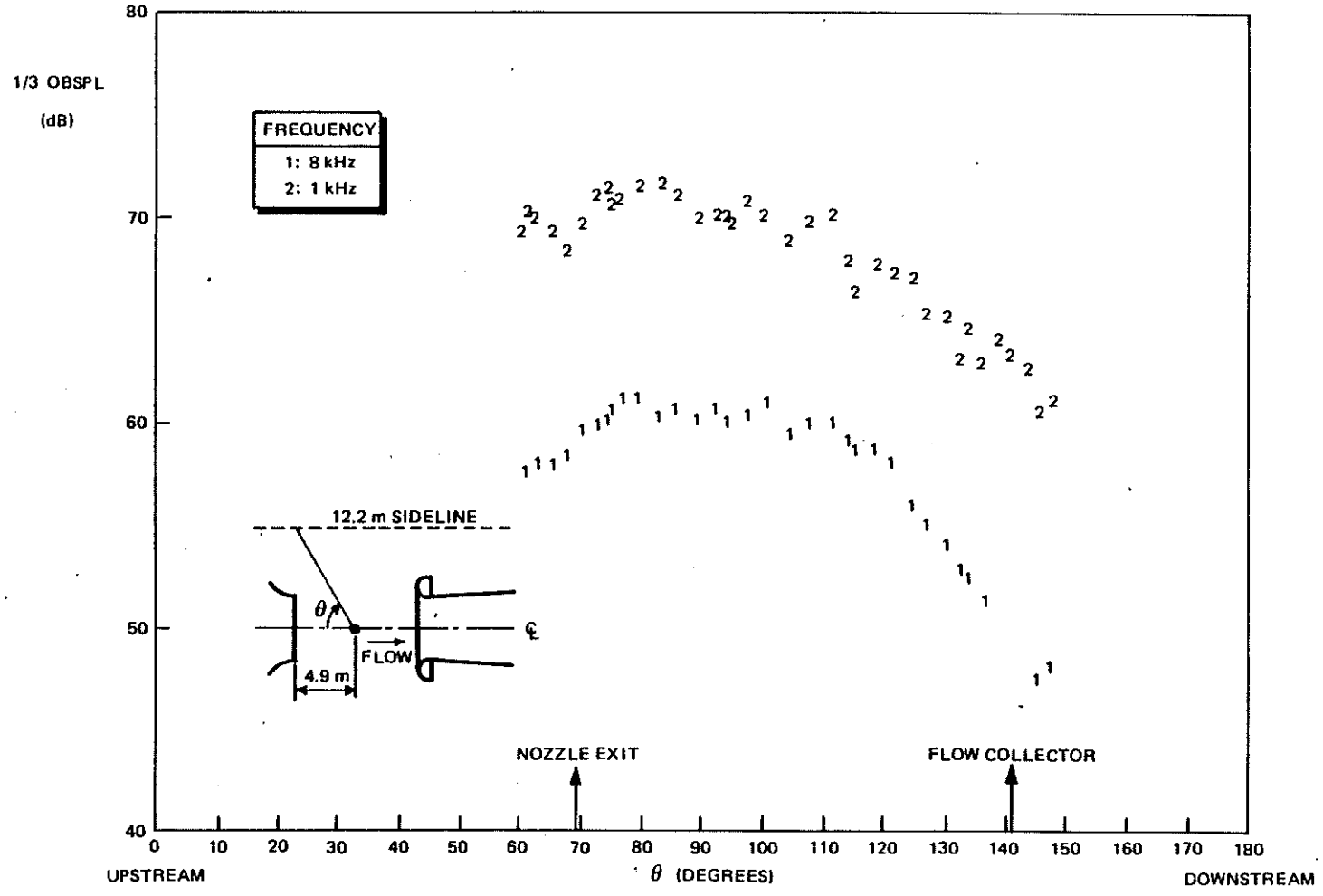

Fig. 24 Background noise at two 1/3 octave frequency bands measured along a 12.2 m sideline, at 80 m/s tunnelspeed

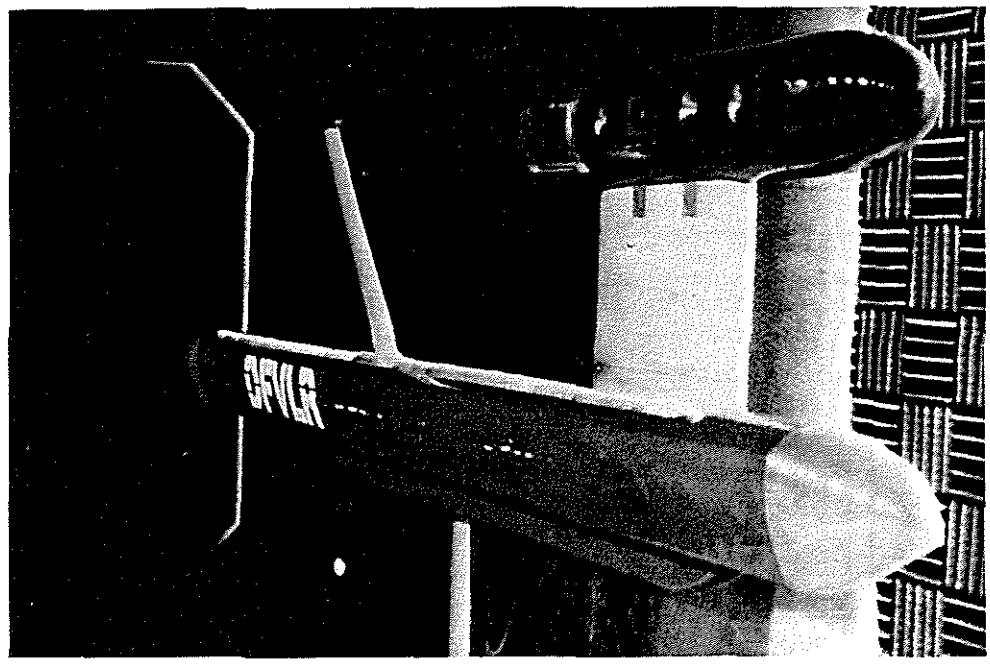

Fig. 25 In-flow traverse and calibrated noise source arrangement

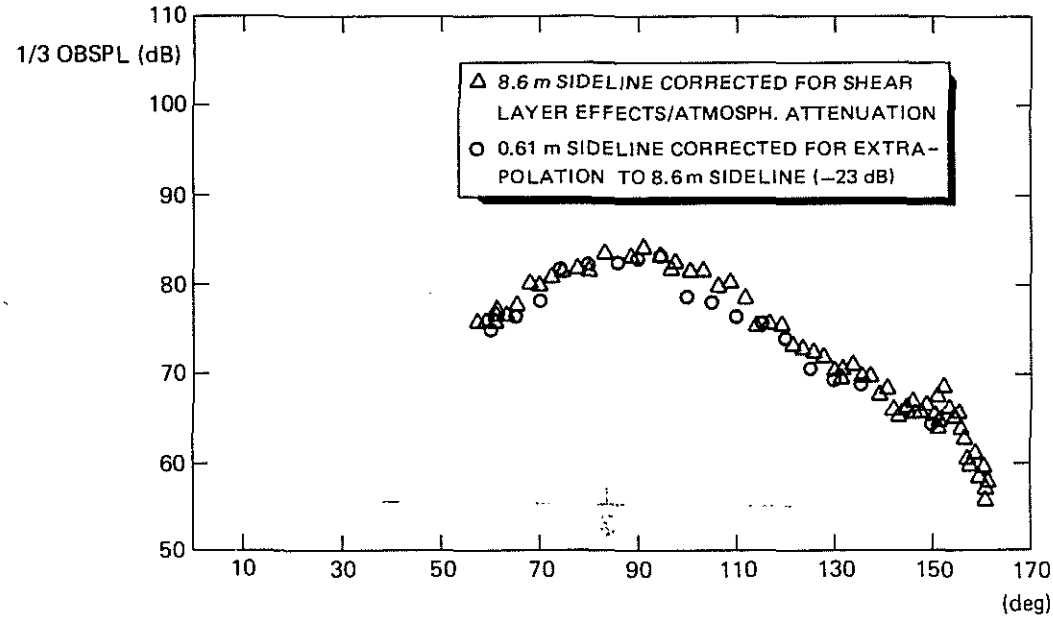

Fig. 26 Directivity plot measured at an 8.6 m out-of-flow sideline compared with extrapolation from a 0.61 m in-flow sideline (1/3 OB at 4000 Hz) at V_o = 65 m/s

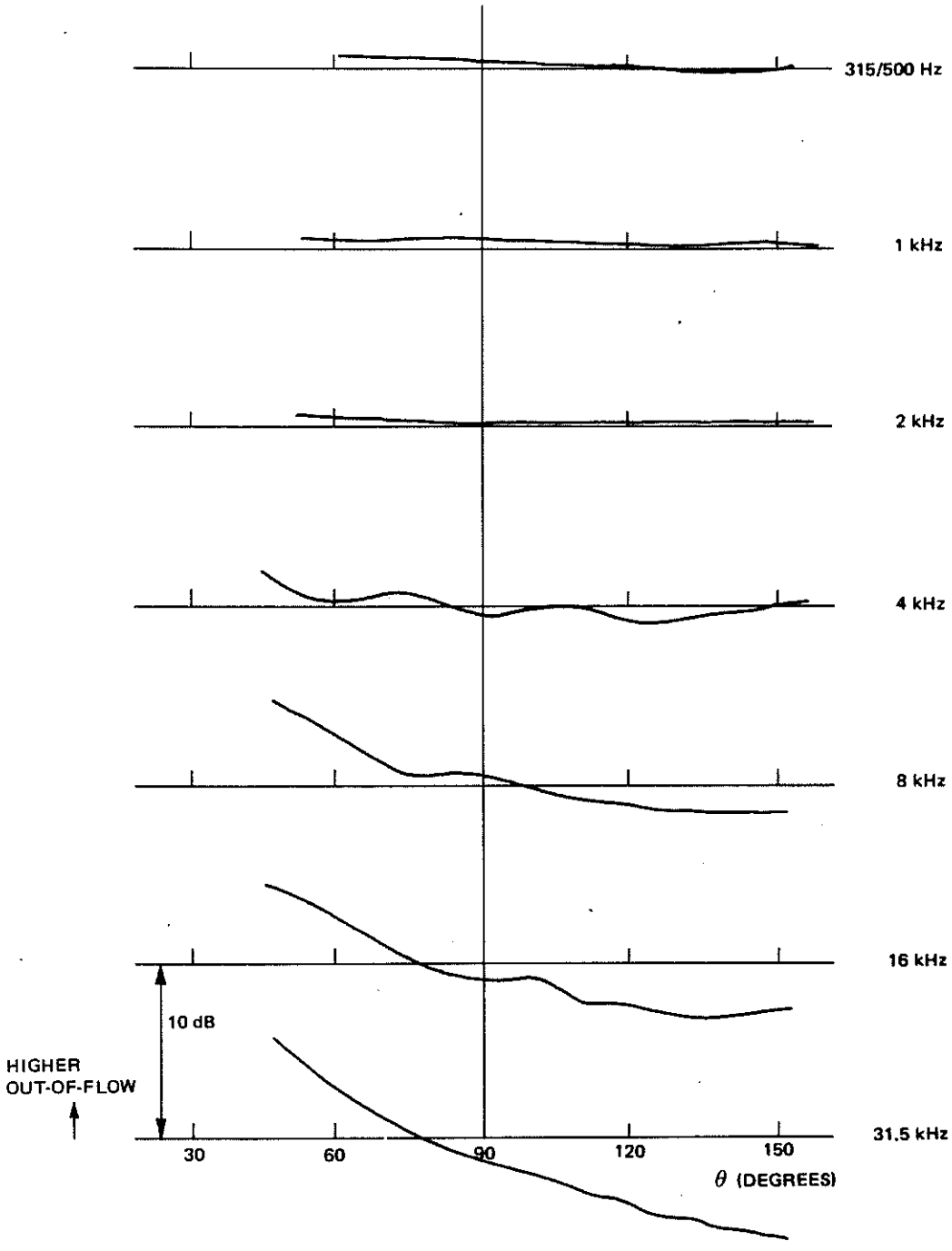

Fig. 27 Difference between in:out-of-flow flight effects, 80 m/s, average of thtee horns

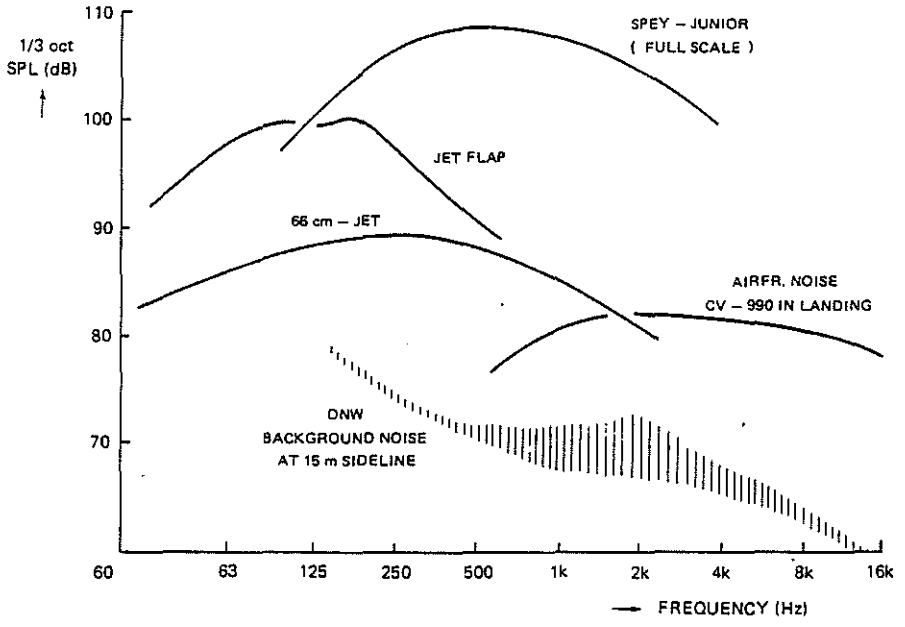

Fig. 28 DNW background noise as compared to some other noise sources at a windspeed of 80 m/s

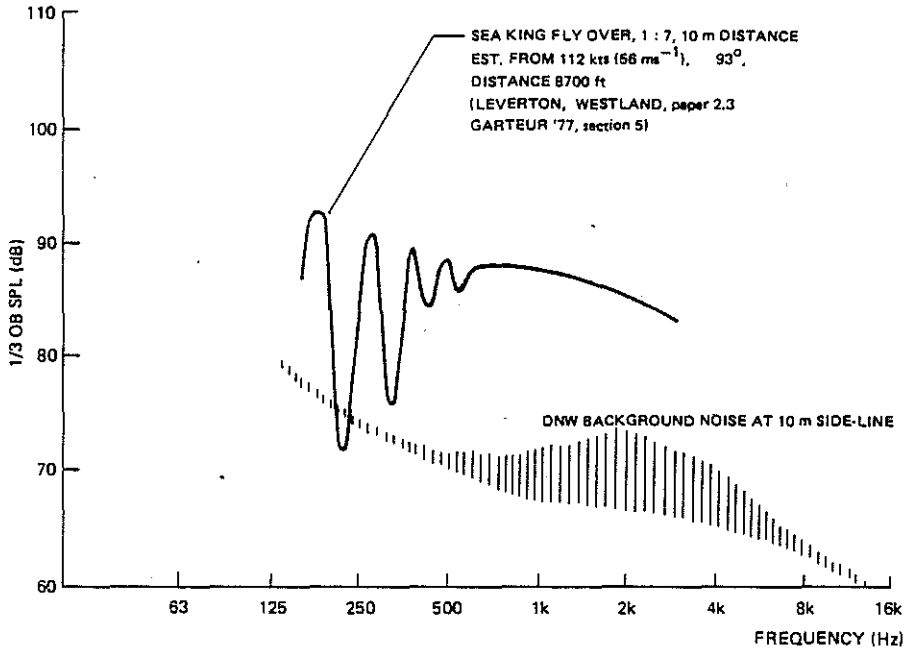

Fig. 29 DNW background noise at a windspeed of 80 m/s^{-1} compared to scaled down fly by noise of sea king at 56 m/s^{-1}

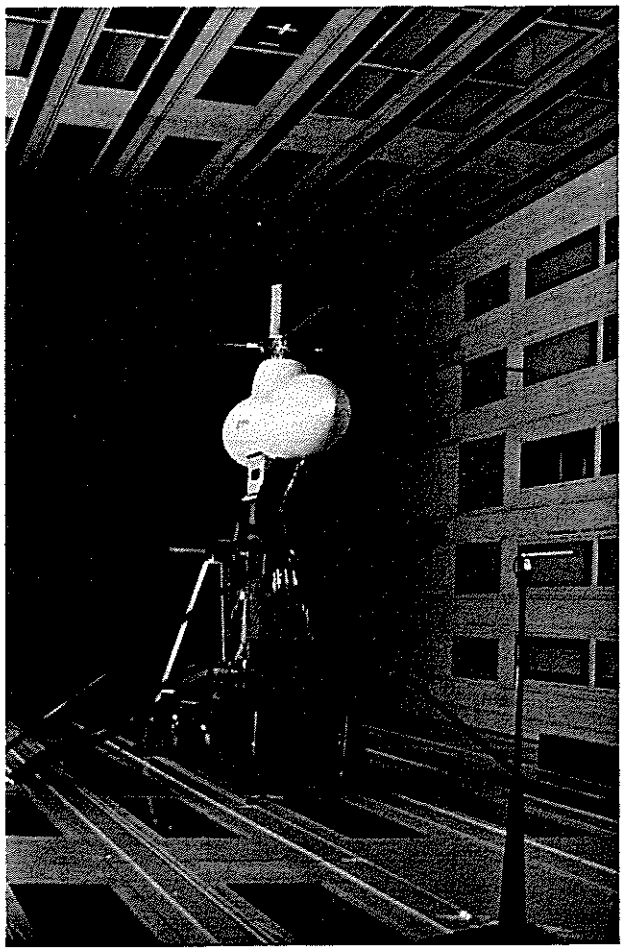

Fig. 30 DFVLR rotor test stand with fuselage model in cabin noise measurements in closed 8 x 6 m^2 test section

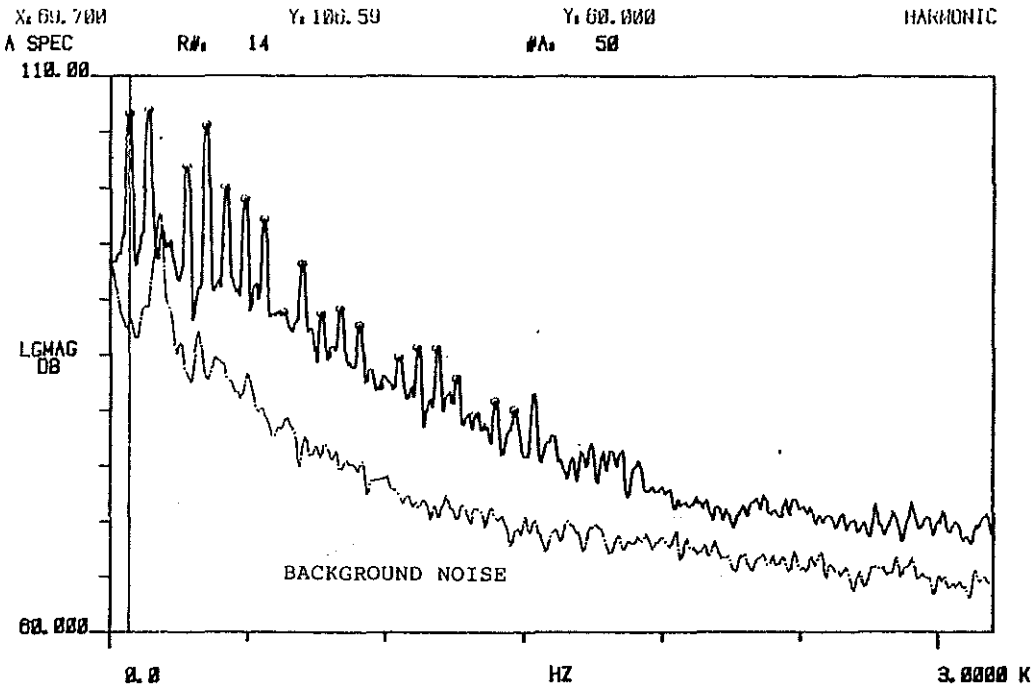

Fig. 31 Narrow band spectrum of main rotor noise (≙ 7 m upstream) under forward flight conditions (rotor thrust 3200 N, wind speed 44 m/s

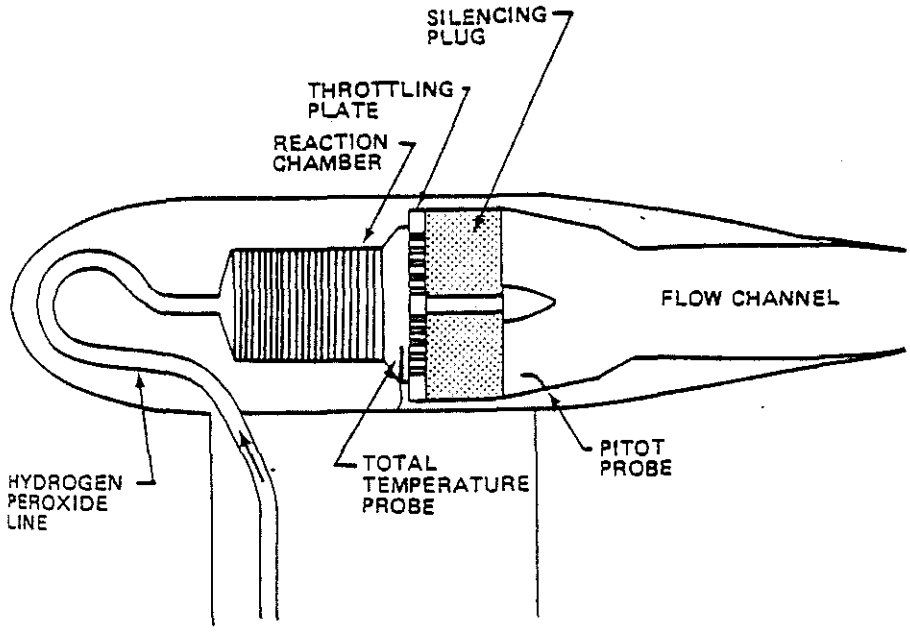

Fig. 32 The DNW 6 cm jet

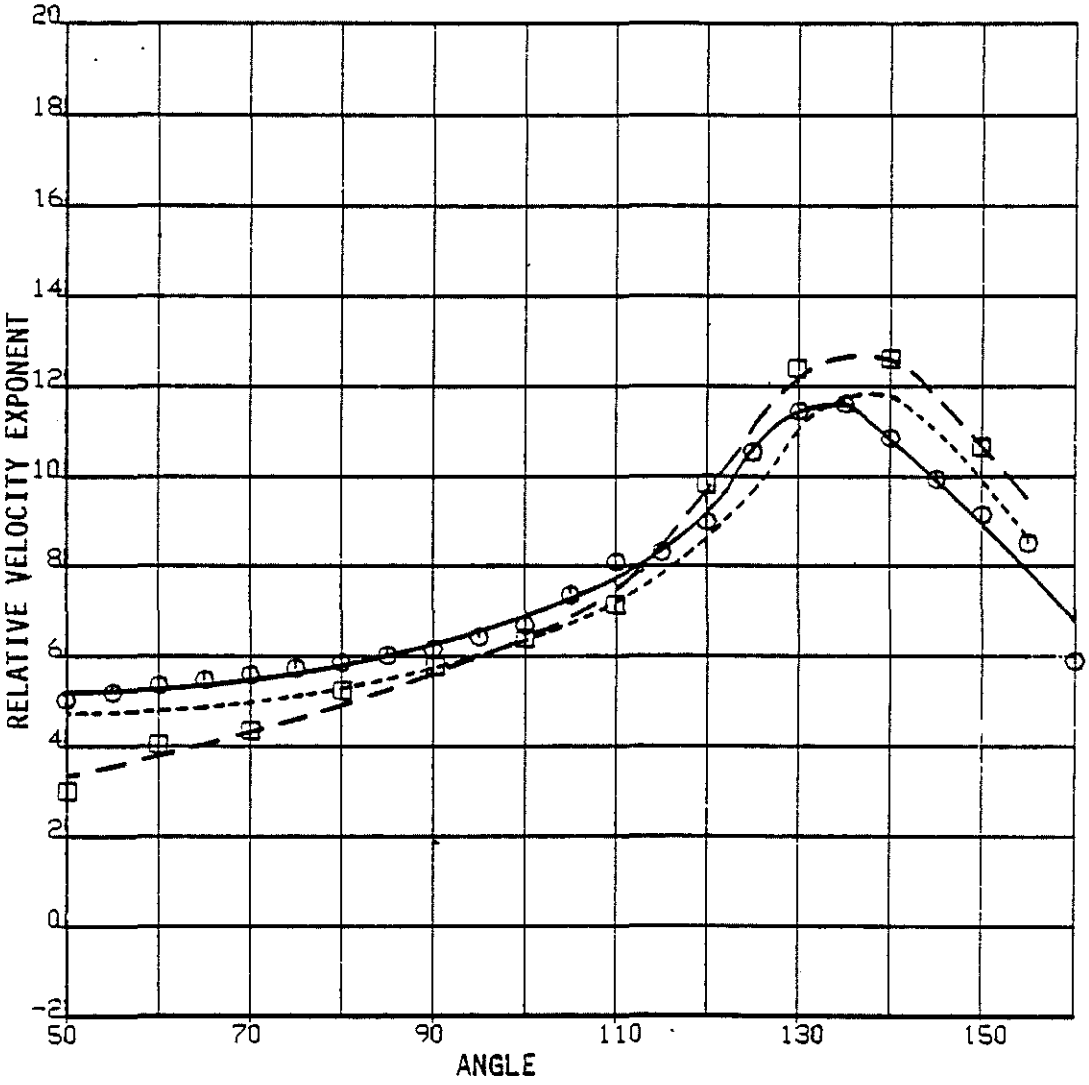

Fig. 33 Relative velocity exponent comparison for NPR = 1.75, tunnel velocity = 80 m/s, and overall SPL

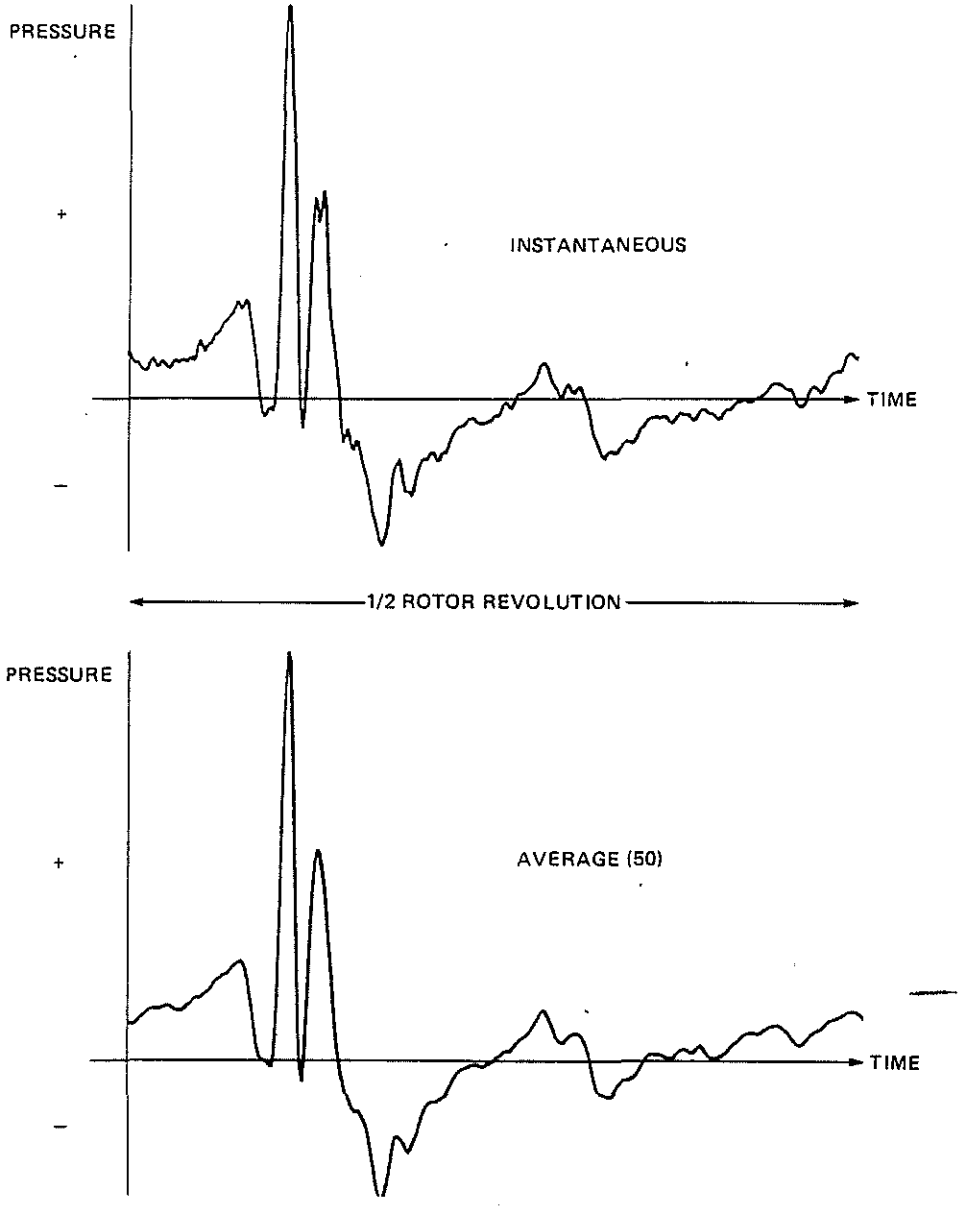

Fig. 34 Acoustic time history of a representative blade-vortex interaction impulsive noise condition (instantaneous & average (50))

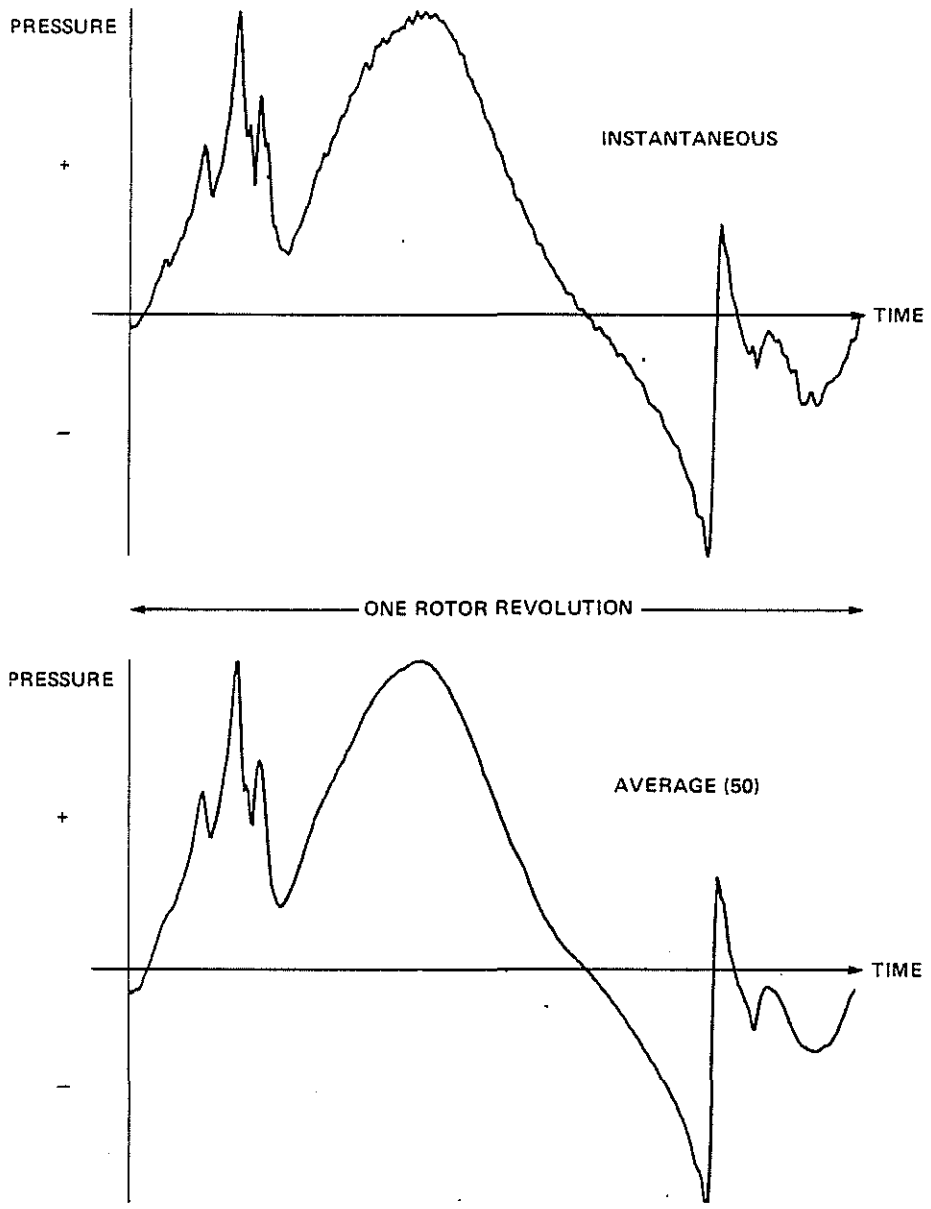

Fig. 35 Pressure time history of a leading-edge pressure transducer (.03C, .965R)

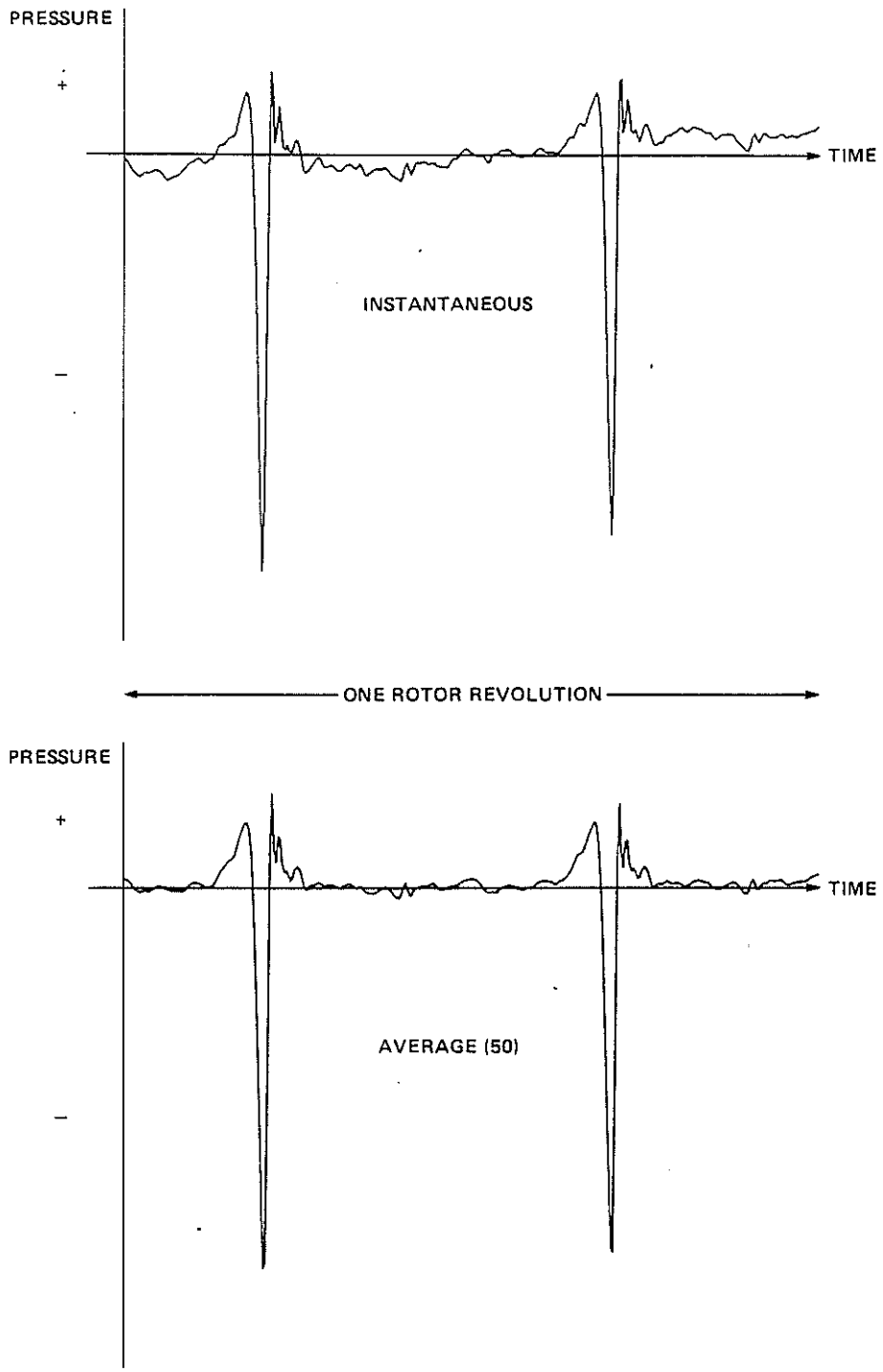

Fig. 36 Acoustic time history of a representative high speed impulsive noise condition. (Microphone located in the plane of and ahead of the rotor.)